迴轉機械之振噪檢測初階訓練課程
智慧型工具機人才培育計畫

訊號分析與理論(初階)

吳 豐 泰

逸奇科技

2011/7/27

內容大綱

- 迴轉機械振動來源與監測診斷
- 資料擷取卡之選用關鍵
- 振動與噪音感測器之簡介
- 振動訊號之分類
- 數位訊號之取樣與離散效應
- 窗型函數與重疊平均
- 常用之頻譜分析技術
- 常見之振動頻譜分類

迴轉機械之振動能量來源與影響[10]

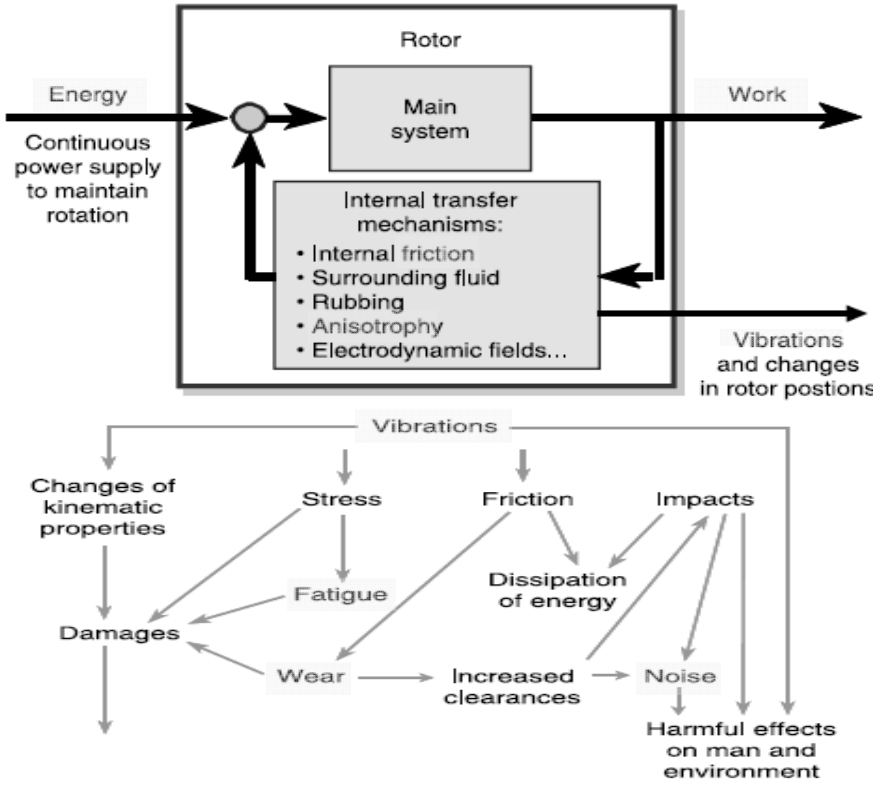

迴轉機械之傳動組成與振動頻譜[12]

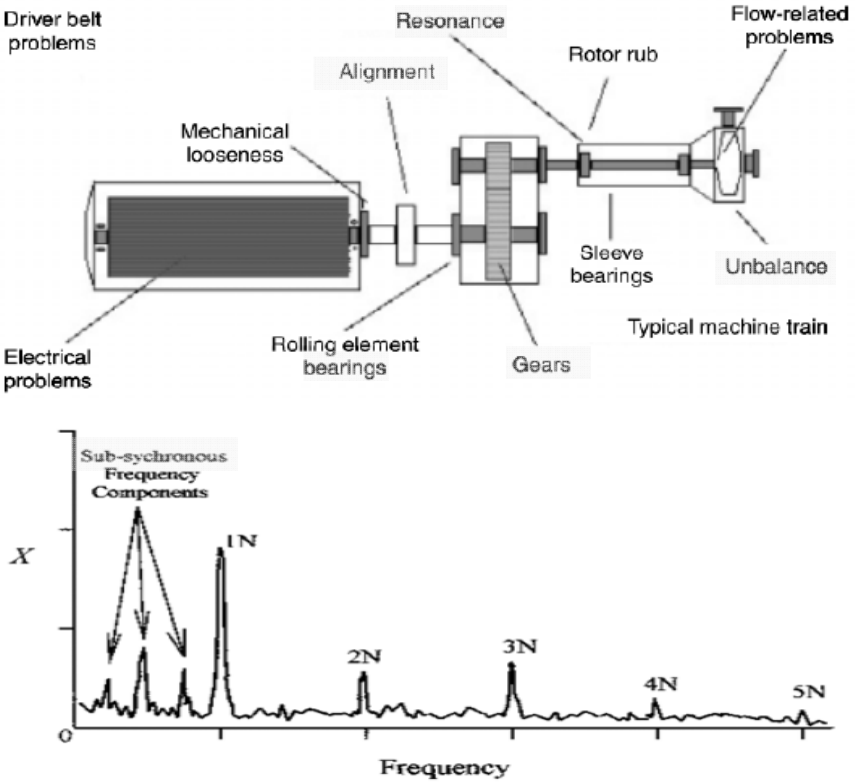

機械運轉壽命與維護分類[10, 12]

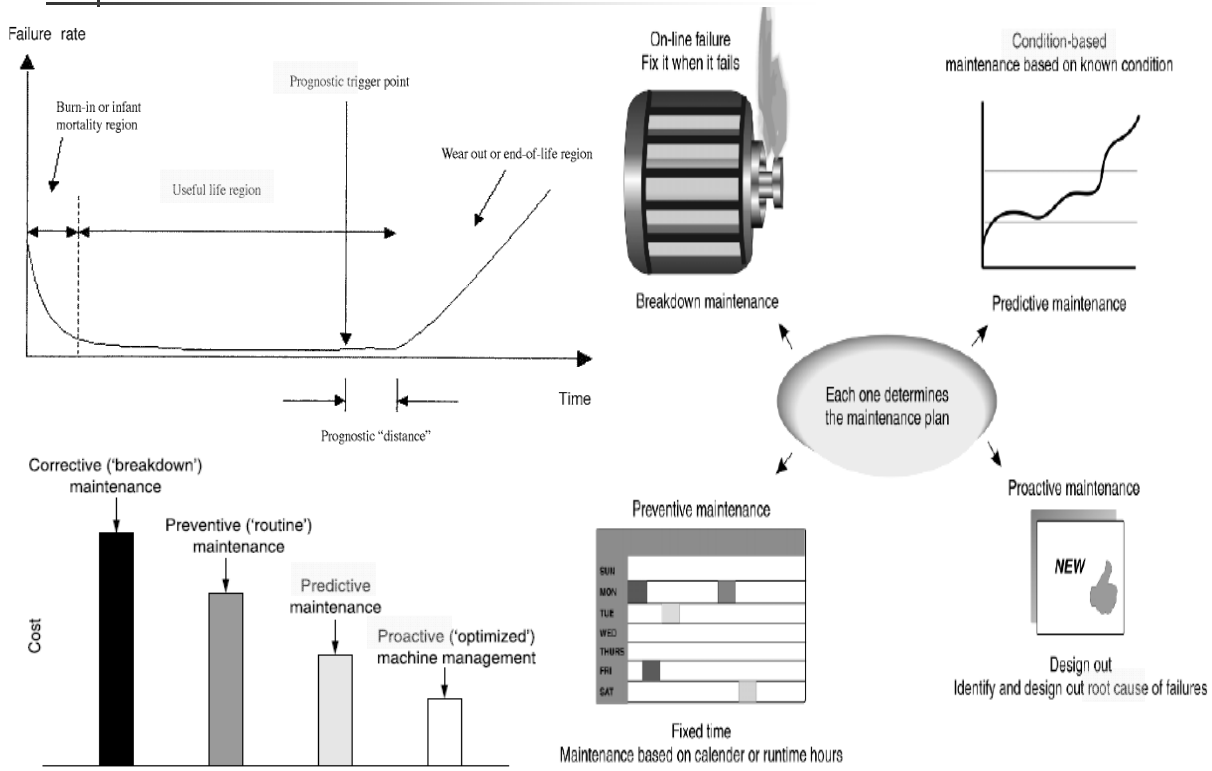

機械系統監測之參數種類[10]

- Condition monitoring
  - Process condition monitoring
    - At operating conditions
      - Efficiency
      - Flow rate
      - Gram mol weight/viscosity/density
      - Rotational speed
      - Electric current/voltage/suction/discharge pressure
      - Temperature
  - Machine condition monitoring
    - At start-up and shutdown
      - Rotor lateral vibrations
      - Rotor torsional vibrations
      - Rotor radial position
      - Thrust (axial) position
      - Casing vibrations
      - Torque
    - At operating conditions
      - Horsepower
      - Heat distribution
      - Lube/oil pressure, flow, and temperature
      - Cracking
      - Noise
      - Oil analysis (wear particles)
      - Perturbation testing
    - At non-operating conditions
      - Nondestructive testing
      - Impact testing
      - Perturbation testing

Signals qualifying for warning/alarm devices

監測狀況之趨勢變化[11]

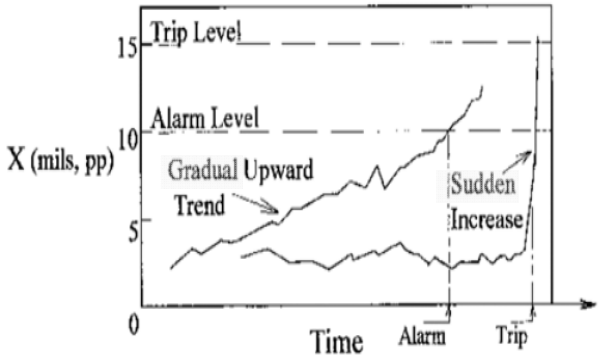

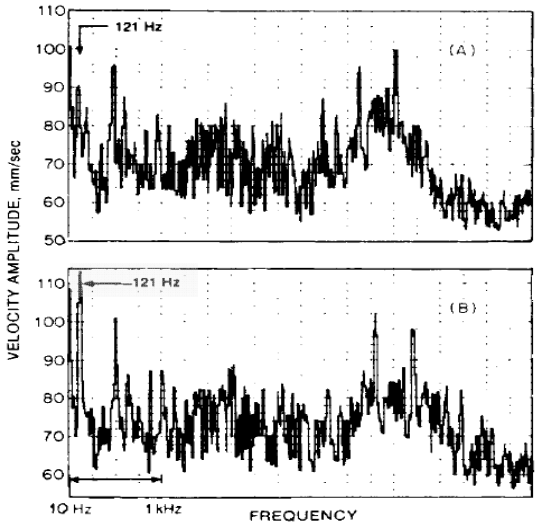

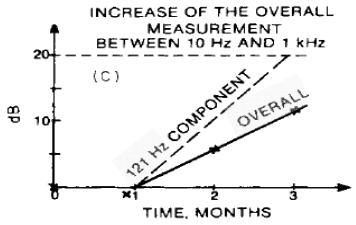

監測狀況之警戒值設定[11]

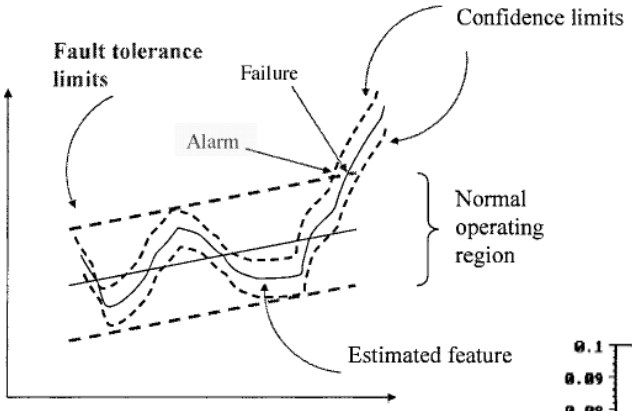

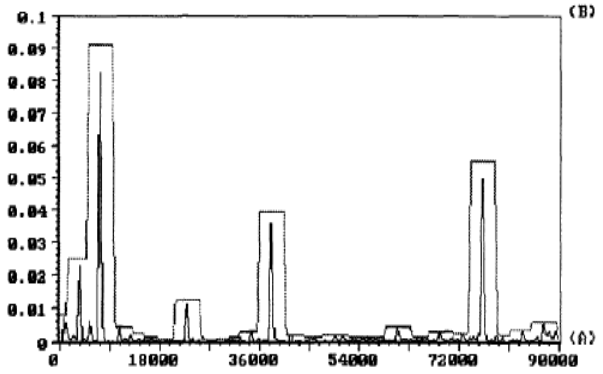

Figure 5-73. Acceptance envelope drawn around acceptable velocity peaks in a compressor spectrum.

ISO 2372機械振動標準等級[12]

ISO 2372 – ISO Guideline for Machinery Vibration Severity					
Ranges of Vibration severity		Examples of quality judgment for separate classes of machines			
Velocity – in/s – Peak	Velocity – mm/s – rms	Class I	Class II	Class III	Class IV
0.015	0.28				
0.025	0.45				
0.039	0.71				
0.062	1.12				
0.099	1.8				
0.154	2.8				
0.248	4.5				
0.392	7.1				
0.617	11.2				
0.993	18				
1.54	28				
2.48	45				
3.94	71				

A – Good
B – Acceptable
C – Still acceptable
D – Not acceptable

PC-based資料擷取流程[7]

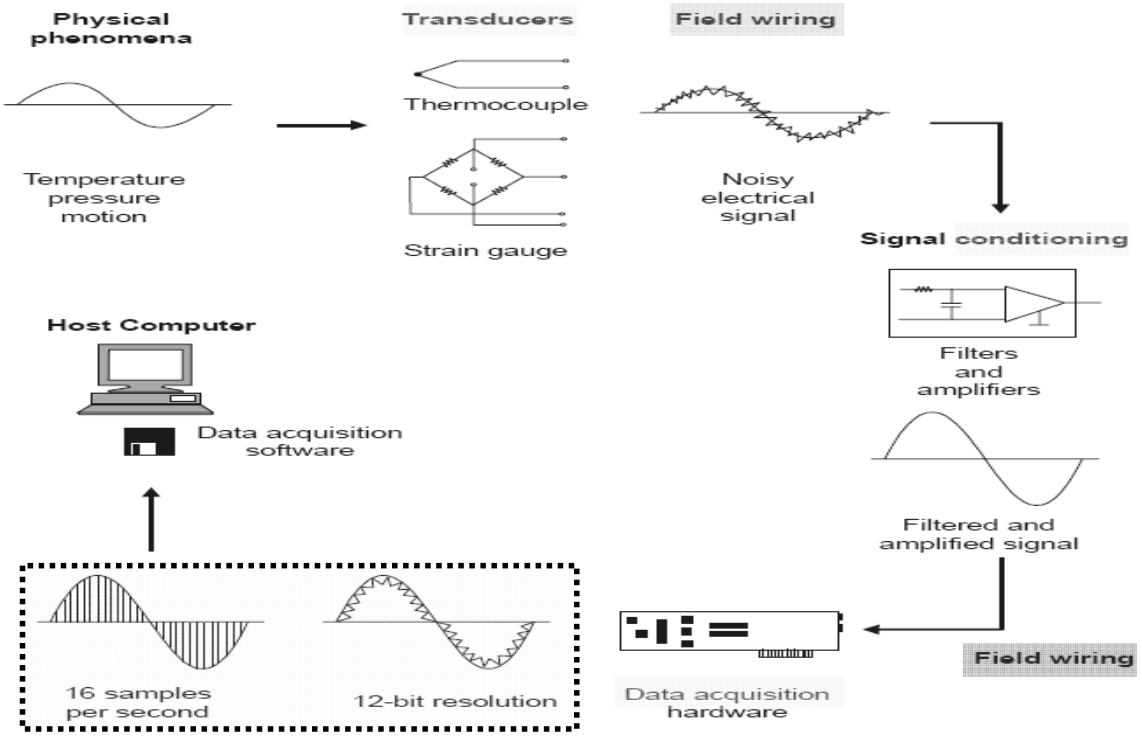

Figure 1.1
Functional diagram of a PC-based data acquisition system

資料擷取卡之數位解析度：類比⇨數位[9]

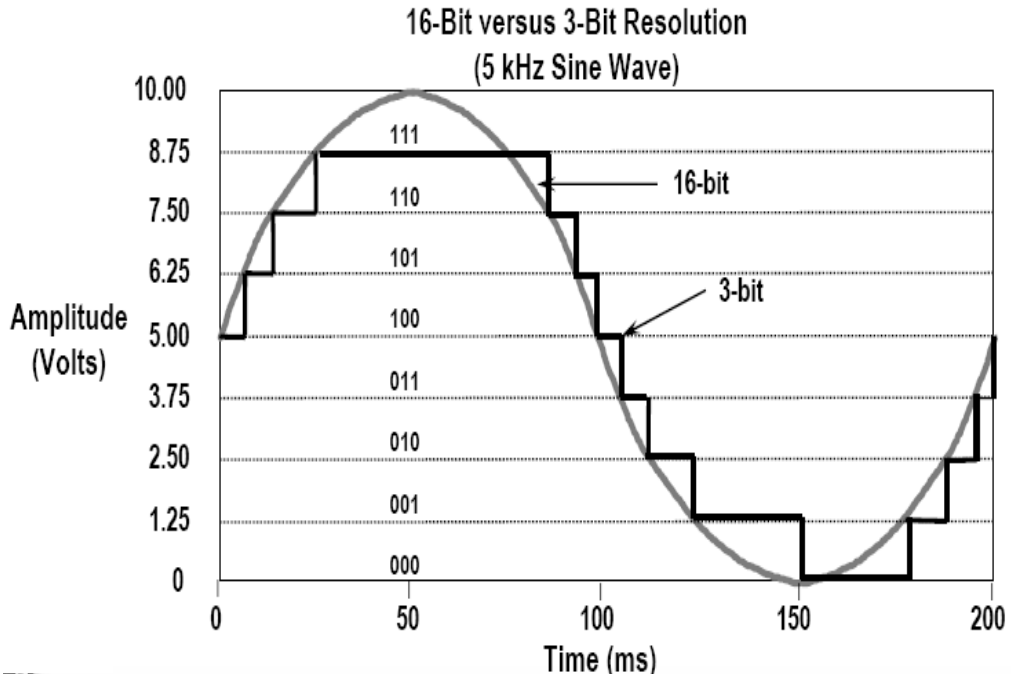

抗鋸齒(Anti-aliasing) 濾波器[9]

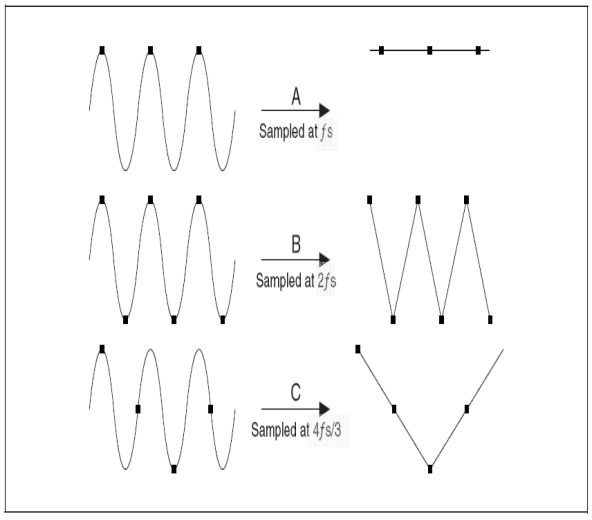

Figure 4-12. Effects of Various Sampling Rates

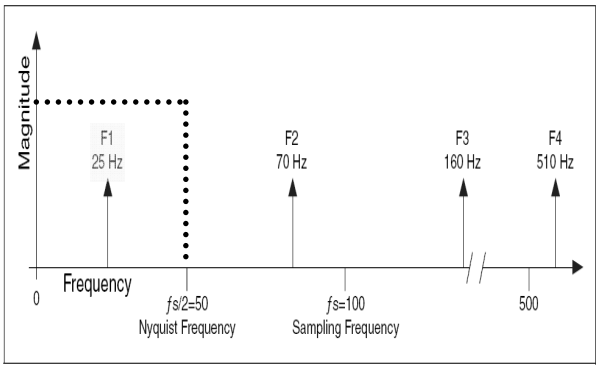

Figure 4-10. Non-Aliased Nyquist Frequency

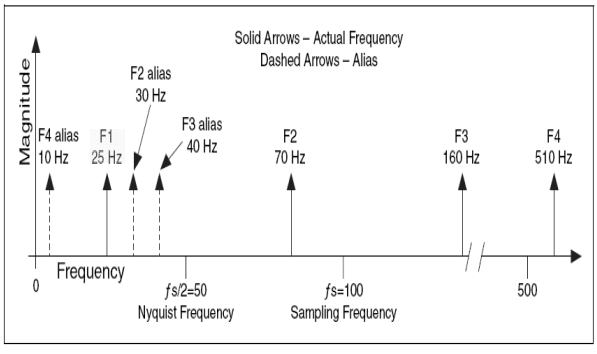

Figure 4-11. Aliased Nyquist Frequency Example

量測感測器分類與連接介面[2, 6, 8]

PROPERTY	SENSOR	ACTIVE/PASSIVE	OUTPUT
Temperature	Thermocouple	Passive	Voltage
	Silicon	Active	Voltage/Current
	RTD	Active	Resistance
	Thermistor	Active	Resistance
Force/Pressure	Strain Gage	Active	Resistance
	Piezoelectric	Passive	Voltage
Acceleration	Accelerometer	Active	Capacitance
Position	LVDT	Active	AC Voltage
Light Intensity	Photodiode	Passive	Current

Figure 1.2.2: Typical sensors and their outputs

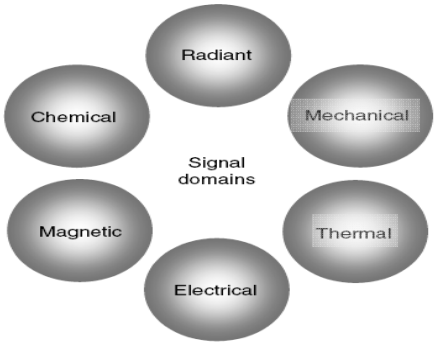

Figure 1.5 Six signal domains

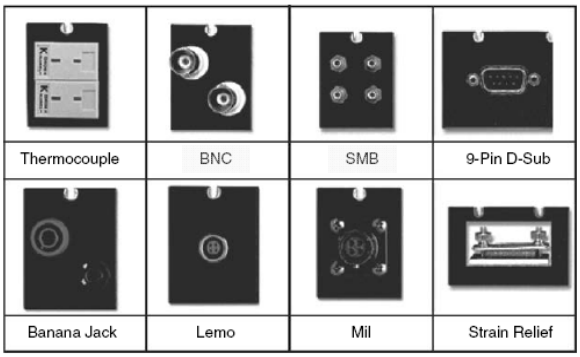

FIGURE 35.4 Examples of signal connectivity options.

麥克風之頻率響應[8]

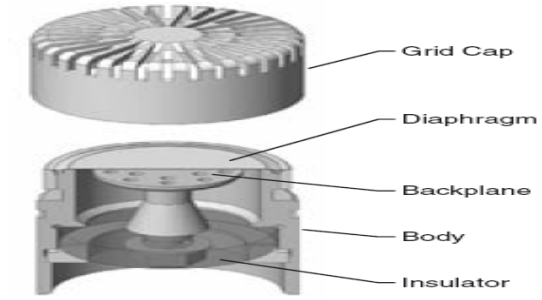

Figure 18.3.1: Measurement microphone, cut-away view.

Figure 18.9.1: Sound intensity probe.

Figure 18.9.2: Array microphone.

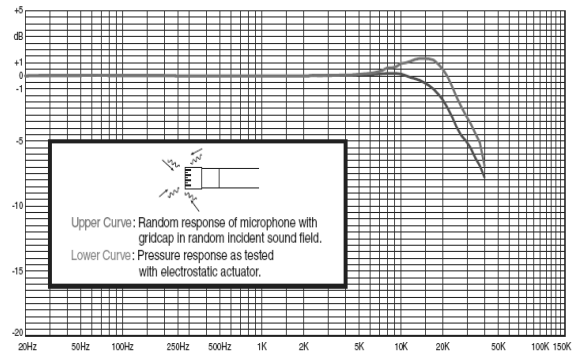

Figure 18.5.1: Frequency response of ½" microphone using an electrostatic actuator (lower curve).

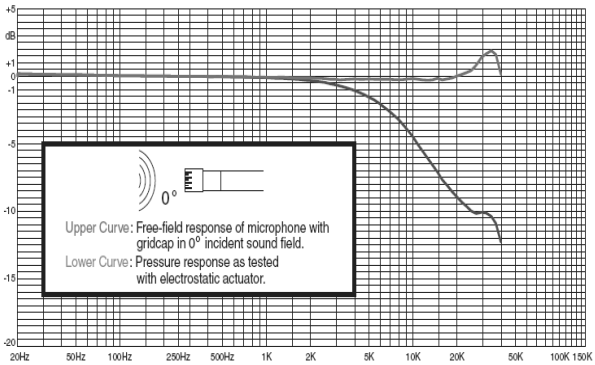

Figure 18.5.4: Free field microphone frequency response.

麥克風之方向性與規格[8]

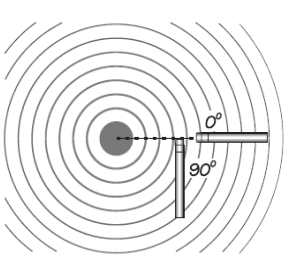

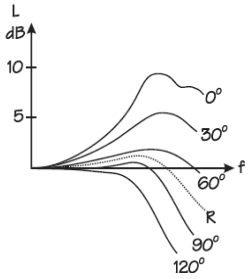

Figure 18.5.3: Free field corrections.

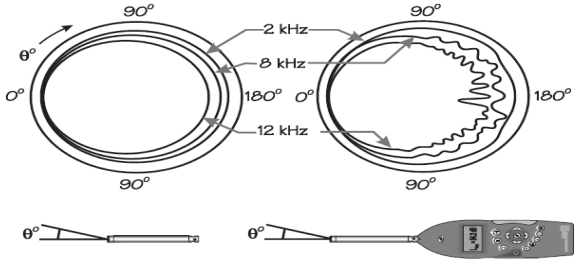

Figure 18.5.5: Directionality of a ½" free field microphone, alone and mounted on a sound level meter.

Pressure and Random Incidence Microphones				
Diameter, Inch	¼	½	½, high sensitivity	1"
Type	P and RI	P and RI	P and RI	Pressure
Sensitivity, mV/Pa	1.3	12	50	50
Low Frequency, Hz*	4	4	3	3
High Frequency, kHz*	70	25	10	8
Thermal Noise, dB	31	18	15	10
3% Distortion Limit, dB	170	160	145	145

** Based on freauency response variation within ±2%.*

Free Field Microphones				
Diameter, in.	¼	½	½, high sensitivity	1"
Sensitivity, mV/Pa	4	12	50	50
Low Frequency, Hz*	4	4	3	3
High Frequency, kHz*	80	40	20	18
Thermal Noise, dB	30	20	15	10
3% Distortion Limit, dB	160	160	145	145

** Based on frequency response variation within ±2%.*

加速規之類型[8]

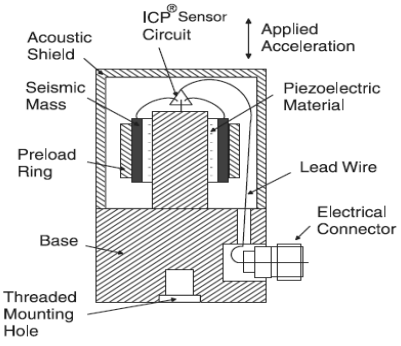

Figure 5.2.6: Shear mode accelerometer.

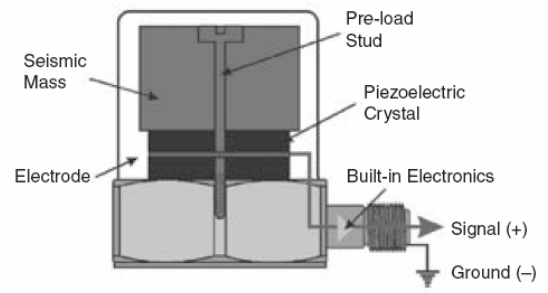

Figure 5.2.8: Compression mode accelerometer.

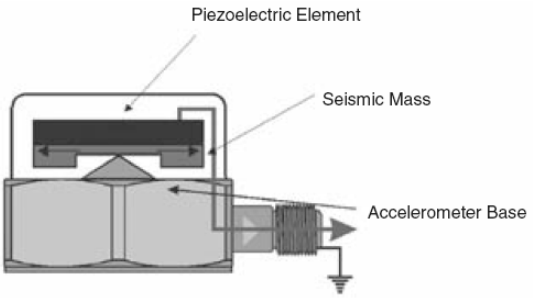

Figure 5.2.7: Flexural mode accelerometer.

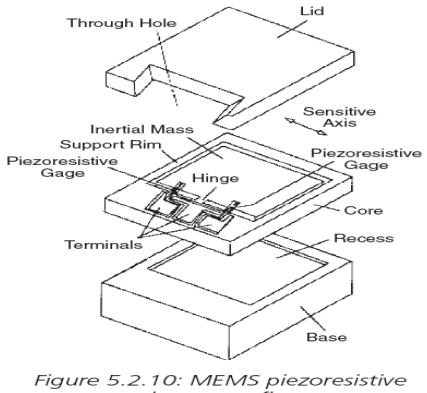

Figure 5.2.10: MEMS piezoresistive accelerometer flexure.

加速規之安裝[8]

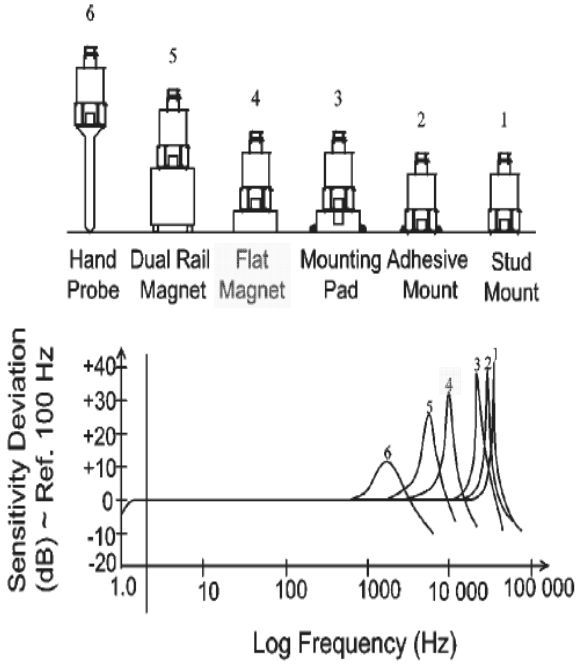

Figure 5.5.1: Relative frequency response of different accelerometer mounting techniques.

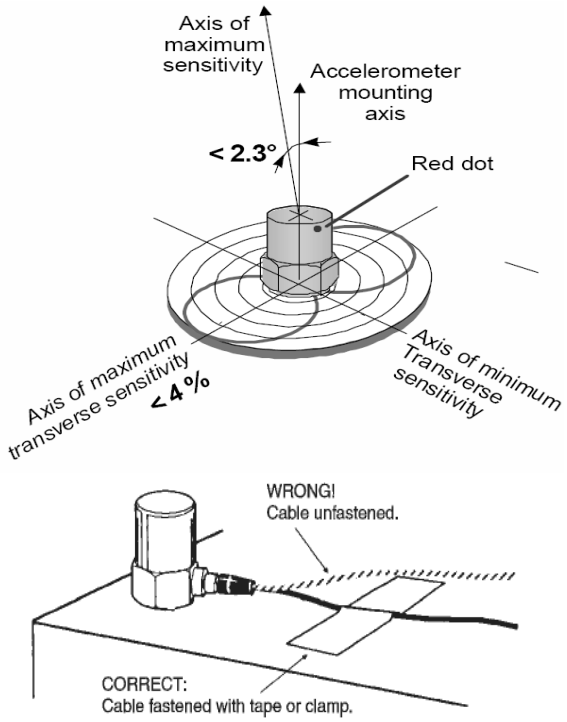

Figure 5.5.2: Cable strain relief of accelerometers.

加速規之選用[8]

Table 13.4.1: Frequency range guidelines [Ref. 4].

Recommended Frequency Spans (Upper Frequency)	
Shaft Vibration	10 × RPM
Gearbox	3 × GMF
Rolling Element Bearings	10 × BPFI
Pumps	3 × VP
Motors / Generators	3 × (2 × LF)
Fans	3 × BP
Sleeve Bearings	10 × RPM

RPM – Revolutions Per Minute
GMF – Gear Mesh Frequency
BPFI – Ball Pass Frequency Inner race
VP – Vane Pass frequency
LF – Line Frequency (60 Hz in USA)
BP – Blade Pass frequency

Table 5.3.2: Typical accelerometer characteristics.

Accelerometer Type	Frequency Range	Sensitivity	Measurement Range	Dynamic Range	Size/weight
IEPE Piezoelectric Accelerometer	0.5 Hz to 50 000 Hz	.05 mV/g to 10 V/g	0.000001 g's to 100,000 g's	~120 dB	.2 Gram to 200 + grams
Charge Piezoelectric Accelerometer	0.5 Hz to 50 000 Hz	.01 pC/g to 100 pC/g	0.00001 g's to 100,000 g's	~110 dB	.14 grams to 200 + grams
Piezoresistive Accelerometer	0 to10000 Hz	0.0001 to 10 mV/g	0.001 to 100000 g's	~80 dB	1 to 100 grams
Capacitive Accelerometer	0 to 1000 Hz	10 mV/g to 1 V/g	0.00005 g's to 1000 g's	~90 dB	10 grams to 100 grams
Servo Accelerometer	0 to 100 Hz	1 to 10 V/g	<0.000001 g's to 10 g's	>120 dB	>50 grams

IEPE與Charge系統之比較[8]

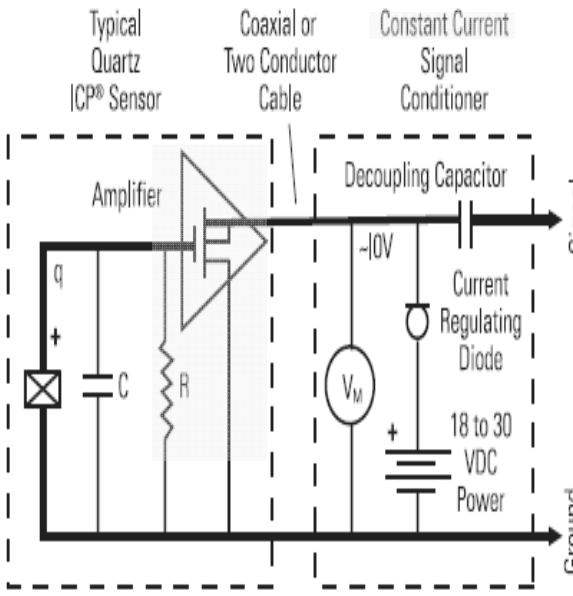

Figure 5.2.3: Typical IEPE system.

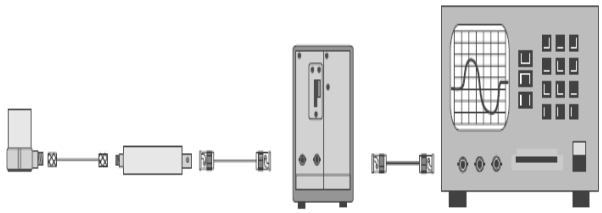

Figure 5.2.4: Typical in-line charge converter system.

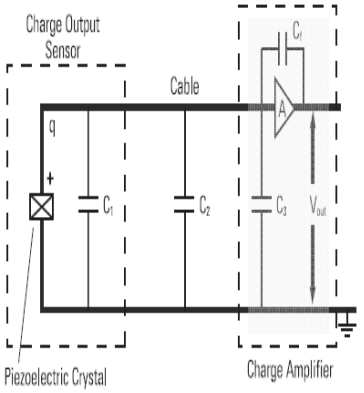

Figure 5.2.5: Laboratory charge amplifier system.

加速規之比較-1[8]

Table 5.3.1: Comparison of accelerometer types.

Accelerometer Type	Advantages	Limitations	Typical Applications
IEPE Piezoelectric Accelerometer	Wide Dynamic Range Wide Frequency Range Durable (High Shock Protection) Powered by Low Cost Constant Current Source Fixed Output Less Susceptible to EMI and RF Interference Can be Made Very Small Less Operator Attention, Training and Installation Expertise Required High Impedance Circuitry Sealed in Sensor Long Cable Driving without Noise Increase Operates into Many Data Acquisition Devices with Built-in Constant Current Input Operates across Slip Rings Lower System Cost per Channel	Limited Temperature Range Max Temperature of 175°C (350°F) Low Frequency Response is Fixed within the Sensor Built in amplifier is exposed to same test environment as the element of the sensor	Modal Analysis NVH Engine NVH Flight testing Body In White Testing Cryogenic Drop Testing Ground Vibration Testing HALT/HASS Seismic Testing Squeak and Rattle Helmet and Sport Equipment Testing Vibration Isolation and Control

加速規之比較-2[8]

Charge Piezoelectric Accelerometer	High operating temperatures to 700°C Wide dynamic Range Wide Frequency Range (Durable) High Shock Protection Flexible Output Simpler Design fewer parts Charge Converter electronics is usually at ambient condition, away from test environment	More Care/attention is required to install and maintain High impedance circuitry must be kept clean and dry Capacitive loading from long cable run results in noise floor increase Powered By Charge Amp which can be complicated and expensive Need to use Special Low Noise Cable	Jet Engine High Temperature Steam Pipes Turbo Machinery Steam Turbine Exhaust Brake

Accelerometer Type	Advantages	Limitations	Typical Applications
Piezoresistive Accelerometer	DC Response Small Size	Lower Shock Protection Smaller Dynamic Range	Crash Testing Flight testing Shock testing
Capacitive Accelerometer	DC Response Better Resolution than PR Type Accelerometer	Frequency Range Average Resolution	Ride Quality Ride Simulation Bridge Testing Flutter Airbag Sensor Alarms
Servo Accelerometer	High Sensitivity Highest Accuracy for Low Level Low Frequency Measurements	Limited Frequency range, High Cost Fragile, Low Shock Protection.	Guidance Applications Requiring little or no DC Baseline Drift

振動訊號分類[14]

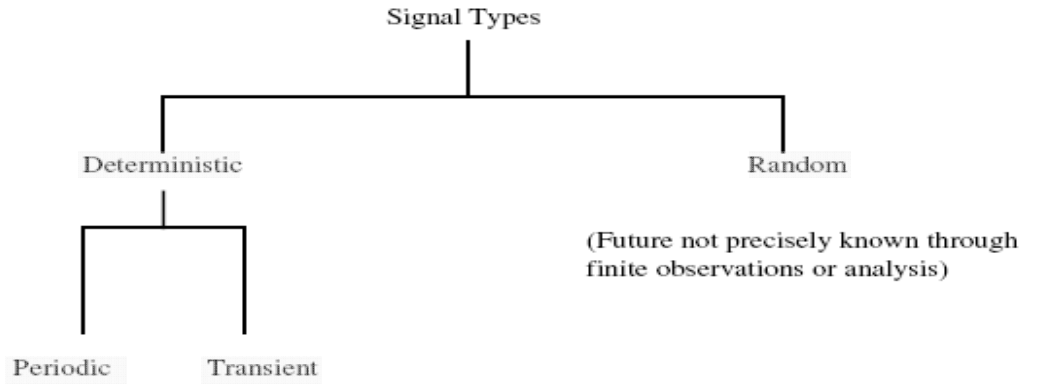

E.g.,
* Blade-passing signal of a turbine at constant speed
* Counter-rotating-mass shaker signal at constant speed
* Step response of an undamped oscillator
* Steady-state response of a damped system to a sine excitation

E.g.,
* Shock wave generated from an impact test with known impulse
* Step response of a damped oscillator
* Response of a variable-speed rotor
* Excitation of a variable-frequency shaker

E.g.,
* Machine tool vibration
* Jet engine noise
* Aerodynamic gusts
* Road irregularity disturbances
* Atmospheric temperature
* Earthquake motions
* Electrical line noise

訊號類型與頻譜[11]

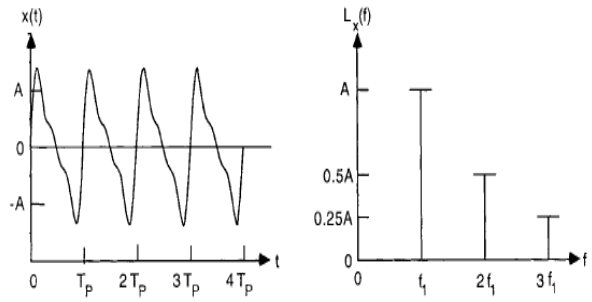

FIGURE 22.2 Time-history and line spectrum for periodic vibration.

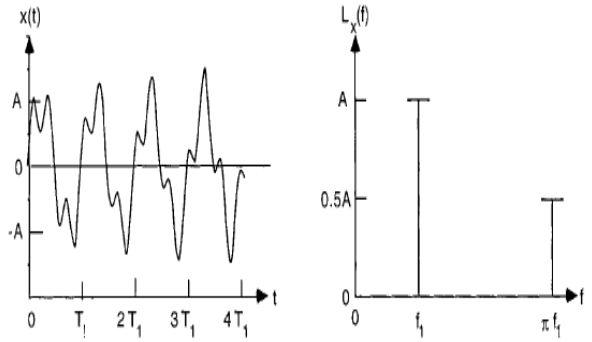

FIGURE 22.3 Time-history and line spectrum for almost-periodic vibration.

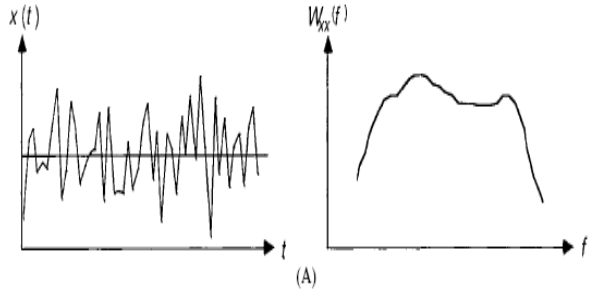

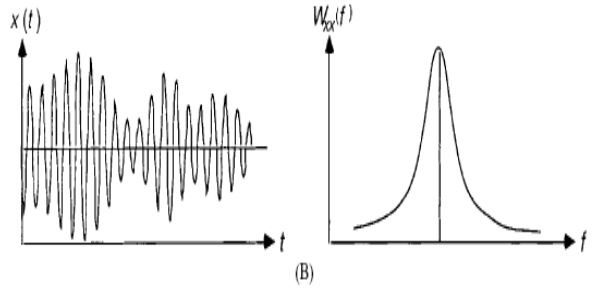

FIGURE 22.6 Time-histories and autospectra for wide-bandwidth (*A*) and narrow-bandwidth (*B*) random vibrations.

取樣頻率之失真效應[11]

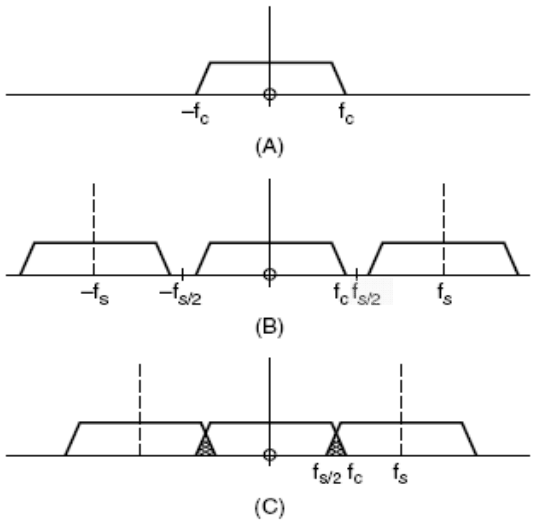

FIGURE 13.10 (*A*) Spectrum of a continuous band-limited signal with maximum frequency f_c. (*B*) Spectrum of digitized signal with sampling frequency $f_s > 2f_c$. (*C*) Spectrum of digitized signal with sampling frequency $f_s < 2f_c$; the hatched area indicates aliased components.

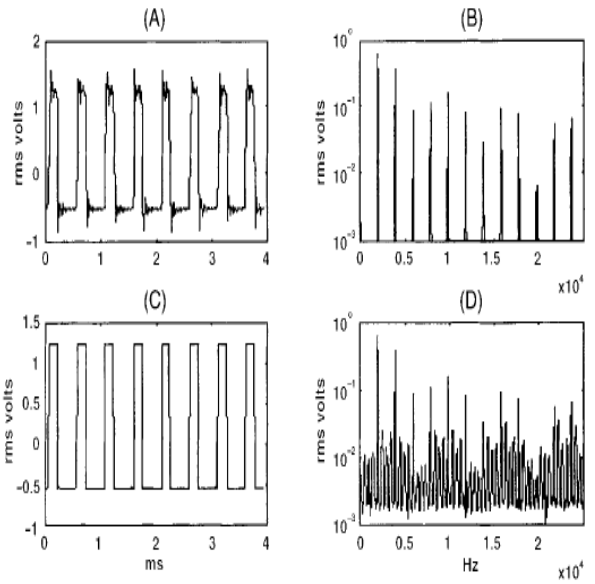

FIGURE 13.11 Effect time signals and spectra of antialiasing filters. (*A*) Time signal with filter. (*B*) Spectrum with filter. (*C*) Time signal without filter. (*D*) Spectrum without filter.

訊號之離散效應[11]

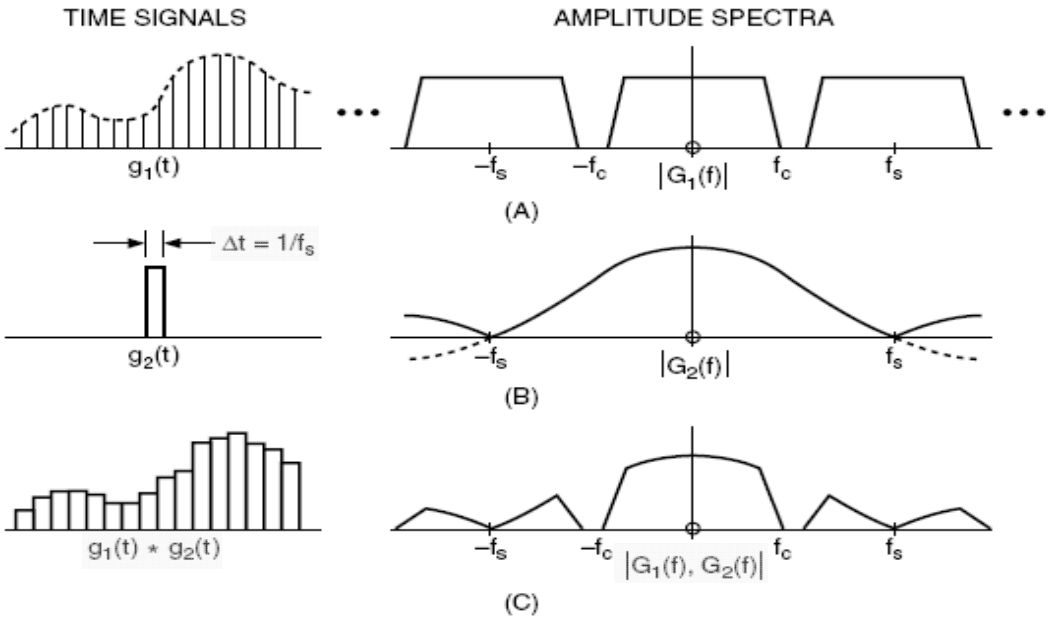

FIGURE 13.12 D/A conversion with constant voltage between samples. (*A*) Digitized time signal and its amplitude spectrum. (*B*) Rectangular pulse length Δt (equal to $1/f_s$) and its amplitude spectrum. (*C*) Convolution of (*A*) and (*B*) and the resulting amplitude spectrum.

窗型函數之效應：時間域[12]

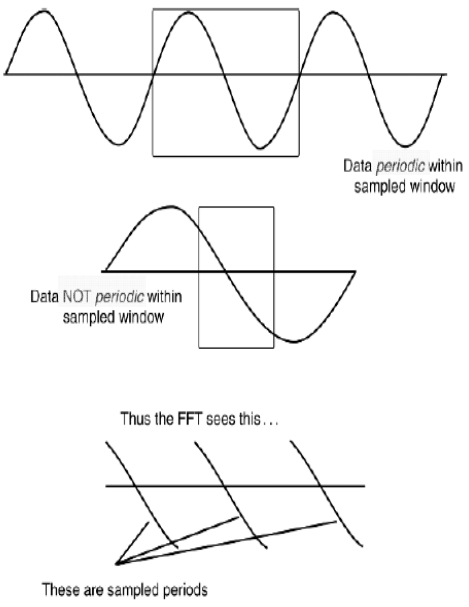

Figure 4.4
The principle of windowing

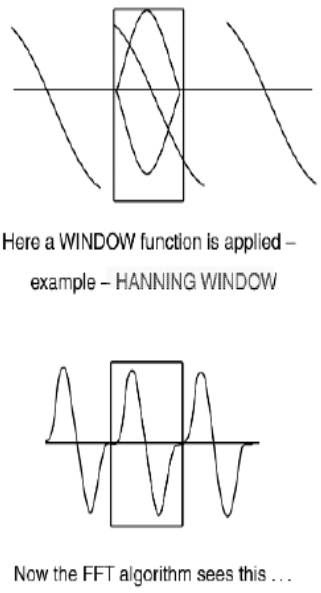

Figure 4.5
Window functions

時間訊號不連續之影響-leakage[11]

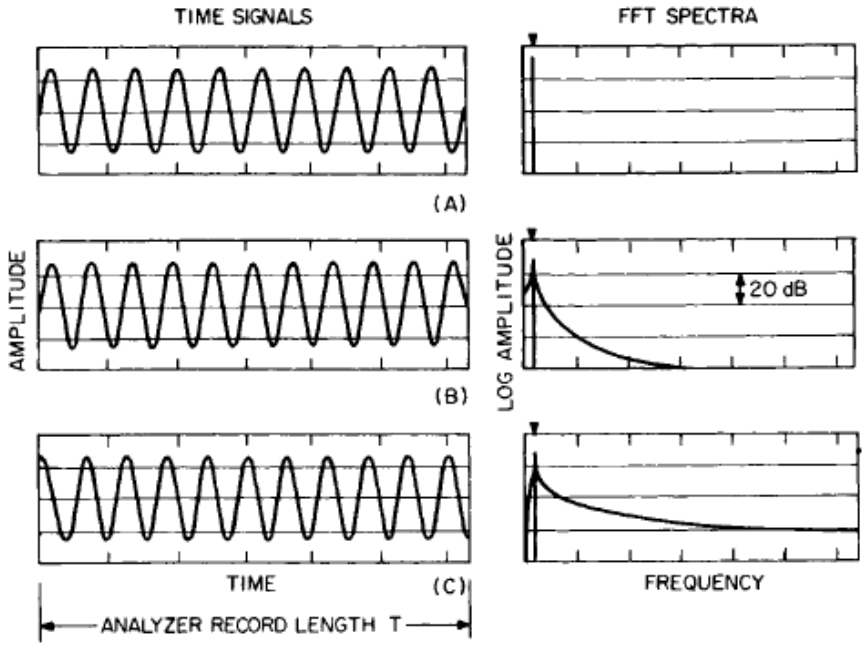

FIGURE 14.9 Time-window effects when analyzing a sinusoidal signal in an FFT analyzer using rectangular weighting. (*A*) Integer number of periods, no discontinuity. (*B*) and (*C*) Half integer number of periods but with different phase relationships, giving a different discontinuity when the ends are joined into a loop.

時間訊號不連續之影響-picket fence[11]

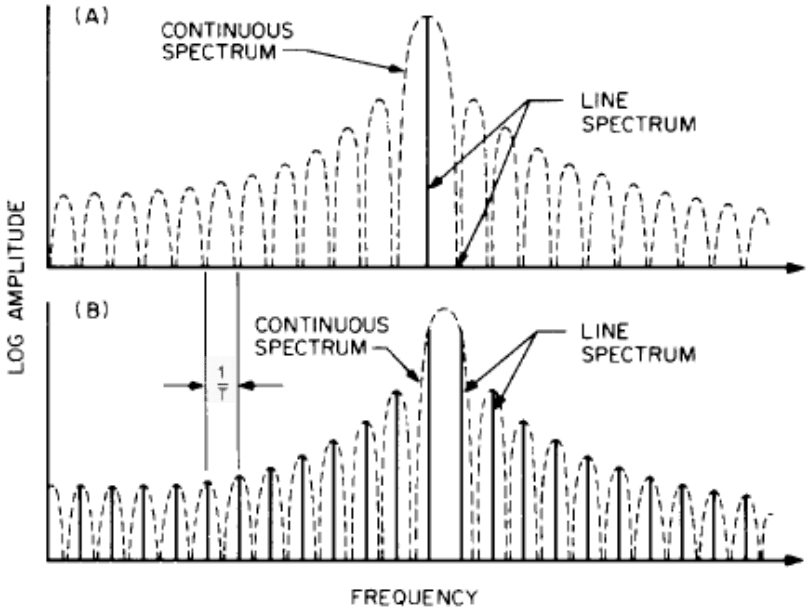

FIGURE 14.10 Frequency sampling of the continuous spectrum of a time-limited sinusoid of length *T*. (*A*) Integer number of periods, side lobes sampled at zero points (compare with Fig. 14.9*A*). (*B*) Half integer number of periods, side lobes sampled at maxima (compare with Fig. 14.9*B* and *C*).

窗型函數之效應：頻率域[12]

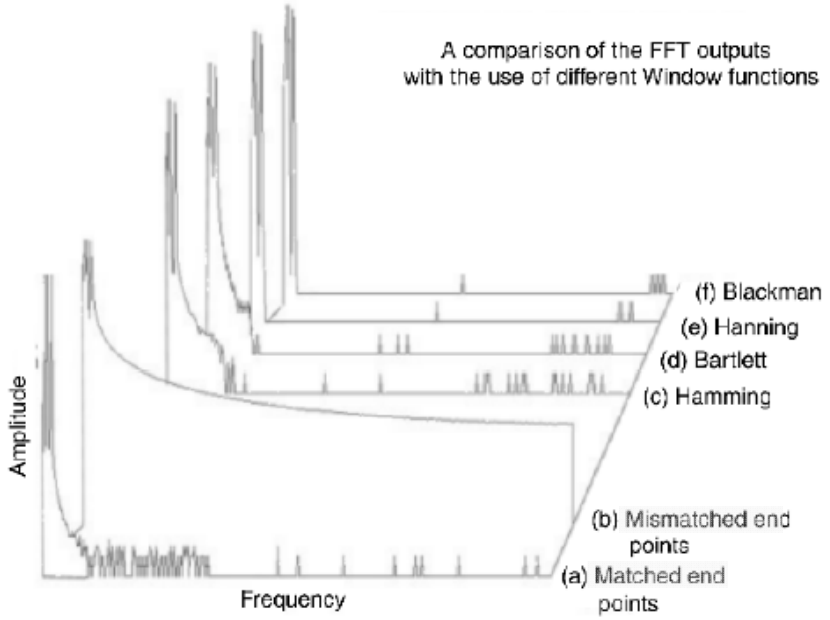

Figure 4.6
Comparison of FFT output

窗型函數之特性比較-1[11]

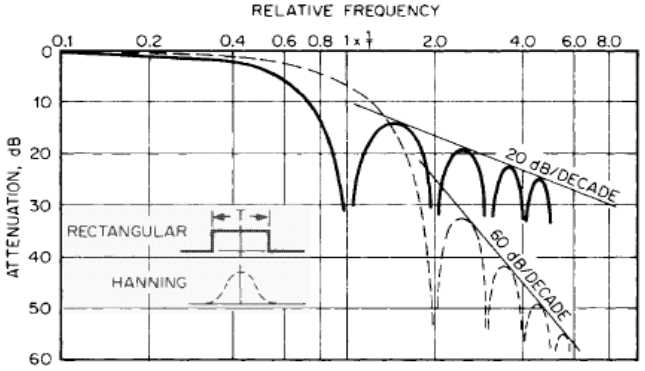

FIGURE 14.12 Comparison of rectangular and Hanning window functions of length T seconds. Full line—rectangular weighting; dotted line—Hanning weighting. The inset shows the weighting functions in the time domain.

TABLE 14.2 Properties of Various Data Windows

Window type	Highest side lobe, dB	Side lobe fall-off, dB/decade	Noise bandwidth*	Maximum amplitude error, dB
Rectangular	−13.4	−20	1.00	3.9
Hanning	−32	−60	1.50	1.4
Hamming	−43	−20	1.36	1.8
Kaiser-Bessel	−69	−20	1.80	1.0
Truncated Gaussian	−69	−20	1.90	0.9
Flattop	−93	0	3.70	<0.1

* Relative to line spacing.

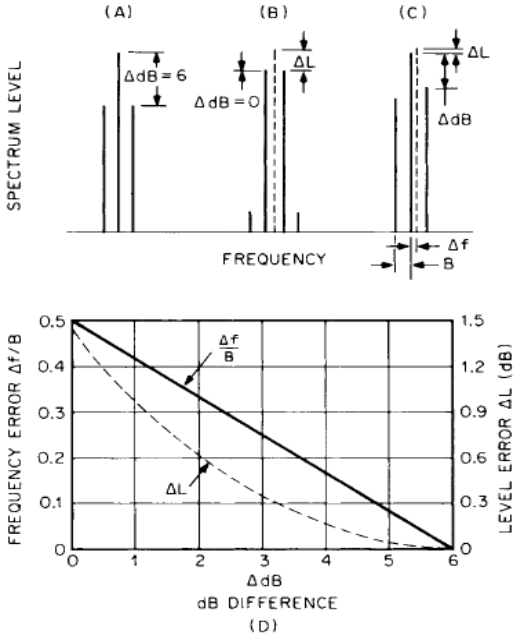

FIGURE 14.14 Picket fence corrections for Hanning weighting, where ΔL = level correction, dB; Δf = frequency correction; Hz; B = line spacing, Hz; ΔdB = difference in decibels between the two highest samples around a peak representing a discrete frequency component. Three examples are shown: (A) Actual frequency coincides with center line. (B) Actual frequency midway between two lines. (C) General situation. Note that the frequency correction $\Delta f/B$ is almost linear.

窗型函數之特性比較-2[11]

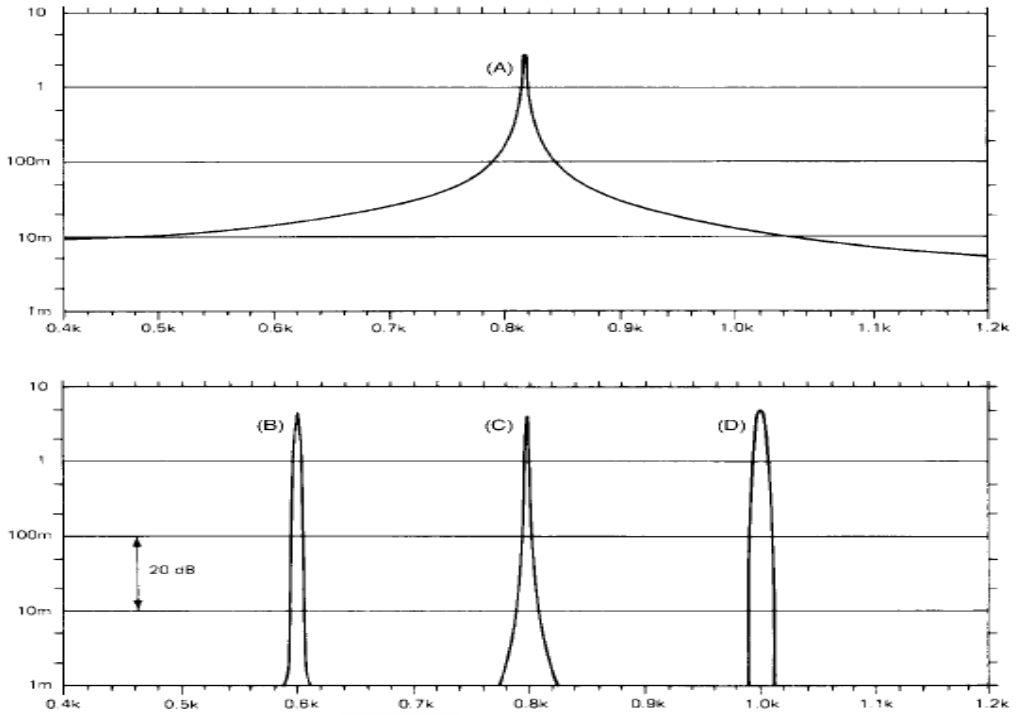

FIGURE 14.13 Comparison of worst-case filter characteristics for rectangular and other weighting functions for an 80-dB dynamic range. (*A*) Rectangular. (*B*) Kaiser-Bessel. (*C*) Hanning. (*D*) Flattop.

時間訊號之重疊與平均-1[11]

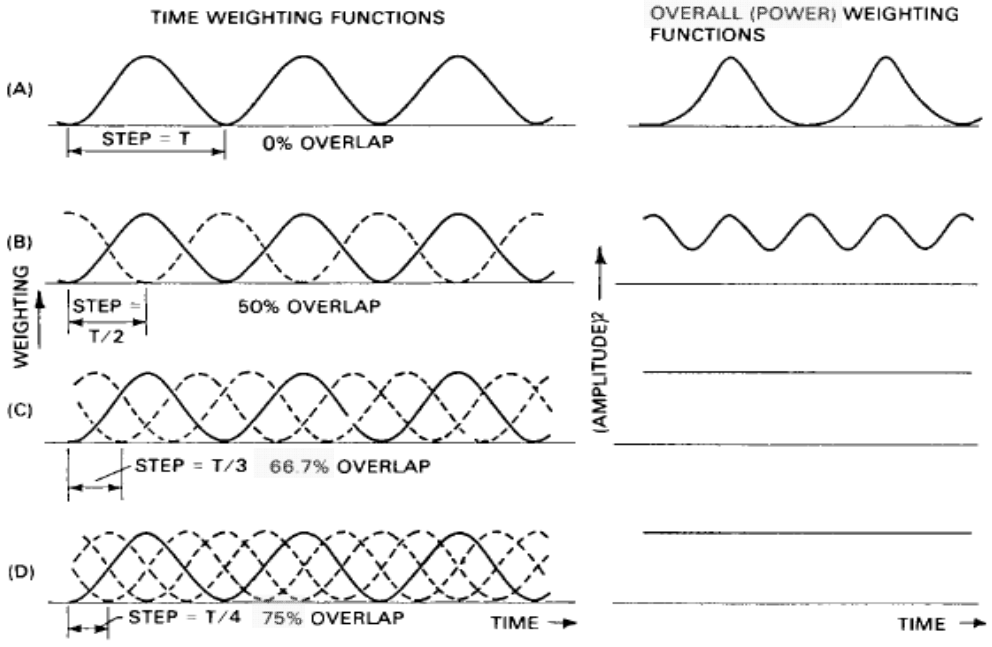

FIGURE 14.20 Overall weighting functions for spectrum averaging with overlapping Hanning windows. (*A*) Zero overlap (step length *T*). (*B*) 50 percent overlap (step length *T*/2). (*C*) 66.7 percent overlap (step length *T*/3). (*D*) 75 percent overlap (step length *T*/4). *T* is the record length for the FFT transform.

時間訊號之重疊與平均-2[11]

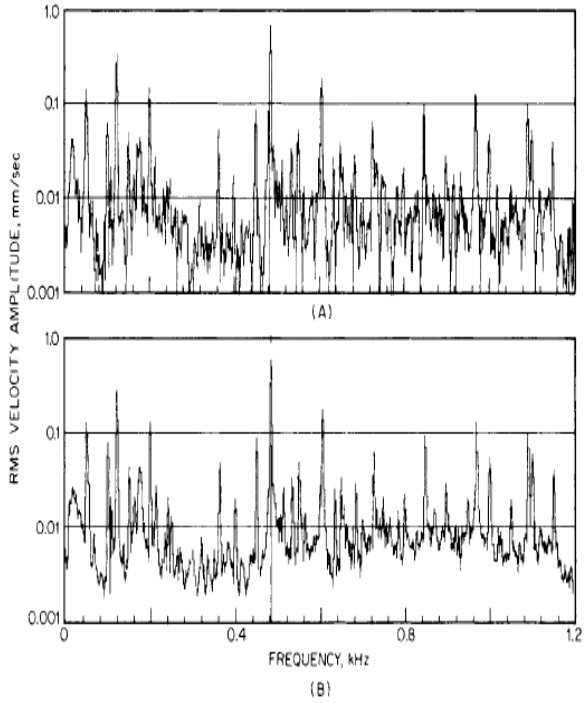

FIGURE 14.18 Effect of averaging with a stationary deterministic signal. (*A*) Instantaneous spectrum (average of 1). (*B*) The linear average of eight spectra.

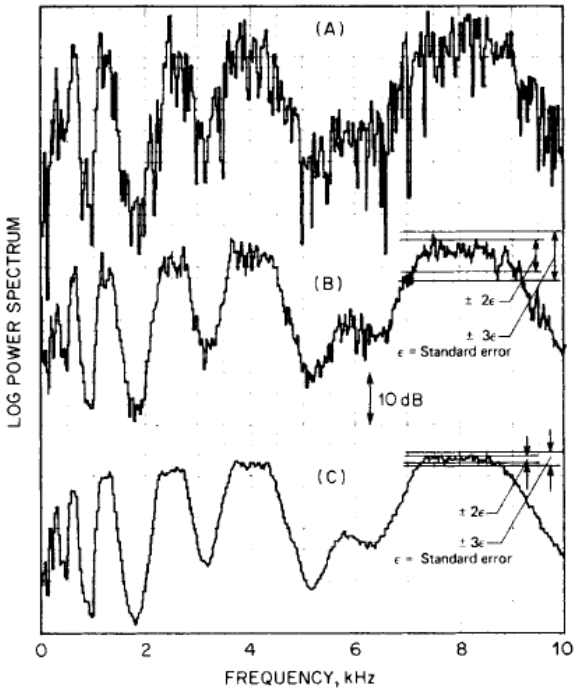

FIGURE 14.19 Effect of averaging with a stationary random signal. (*A*) Instantaneous spectrum. (*B*) Average of eight spectra. (*C*) Average of 128 spectra.

常用之頻譜分析技術[11]

TABLE 16.5 Typical Applications of the Various Analysis Techniques

Technique	Application	Fault/machine
Zoom	Separation of closely spaced components Improvement of signal-to-noise ratio, separation of resonances from pure tones	Electrical machines, gearboxes, turbines
Phase	Operational deflection shapes Detection of developing cracks in shafts Balancing	
Time signal	Waveform visualization for identification of distortion	Rubbing, impacts, clipping, cracked teeth
Cepstrum	Identification and separation of families of harmonics Identification and separation of families of sidebands	Rolling elements bearing, bladed machines, gearboxes
Envelope analysis	Amplitude demodulation Observation of a low-frequency amplitude modulation happening at high frequency	Rolling element bearing, electrical machines, gearboxes
Dynamic crest factor	Calculation of high-pass filtered signals	Faults in low-speed machines
Synchronous time averaging	Improving signal-to-noise ratio Waveform analysis Separating effects of adjacent machines Separating effects of different shafts Separating electrically and mechanically induced vibrations	Electrical machines, reciprocating machines, gearboxes, etc.
Impact testing	Resonance testing	Foundations, bearings, couplings, gears
Scan analysis	Analysis of nonstationary signals	Fast run-up/coast down

時間訊號之同步平均-1[11]

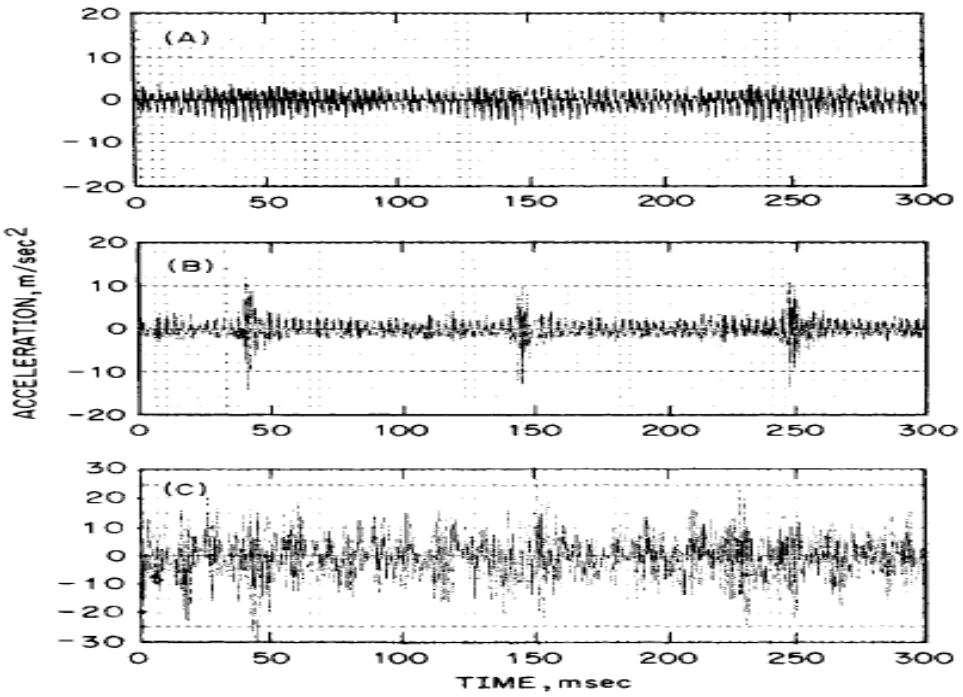

FIGURE 14.30 Use of signal enhancement in gear fault diagnosis. (*A*) Enhanced signal (120 averages) for a gear in normal condition. (*B*) Enhanced signal (120 averages) for a similar gear with a local fault. (*C*) Section of raw signal corresponding to (*B*).

時間訊號之同步平均-2[13]

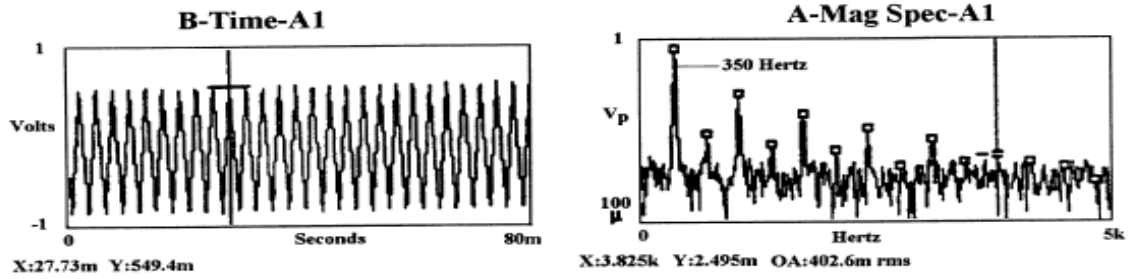

Figure 28.1 Unaltered time waveform (left) and standard averaged spectrum (right) after 1000 averages.

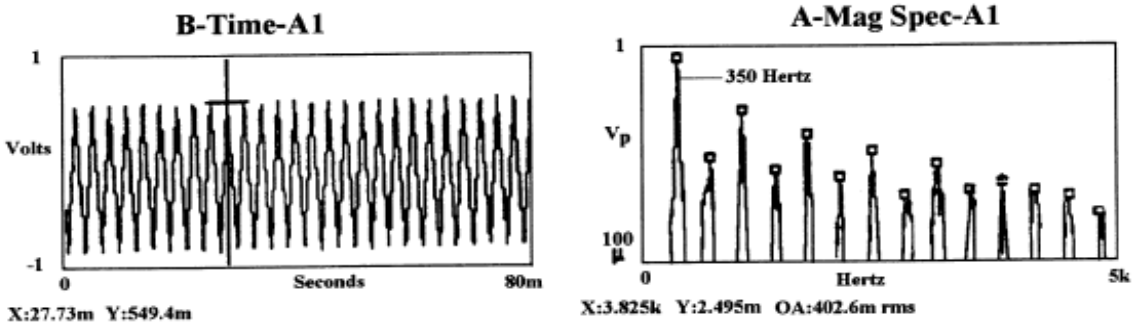

Figure 28.2 Sync averaged time waveform (left) and sync spectrum (right) after 10,000 averages.

Zoom FFT[11]

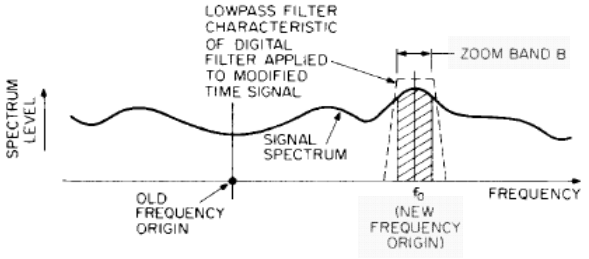

FIGURE 14.16 Principle of real-time zoom, using a low-pass filter to filter out the portion of the original signal in the zoom-band of width B. Prior to this, the frequency origin is shifted to frequency f_0 (the desired center frequency of the zoom-band) by multiplying the (digitized) time signal by $e^{-j2\pi f_0 t}$.

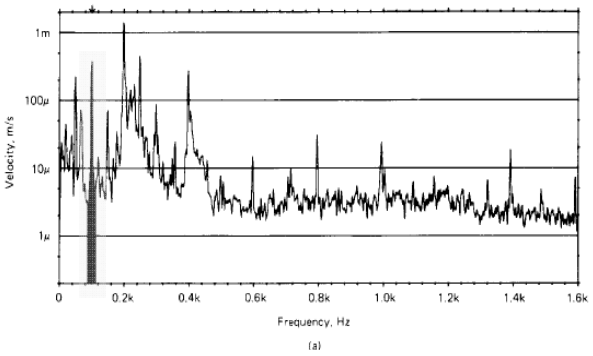

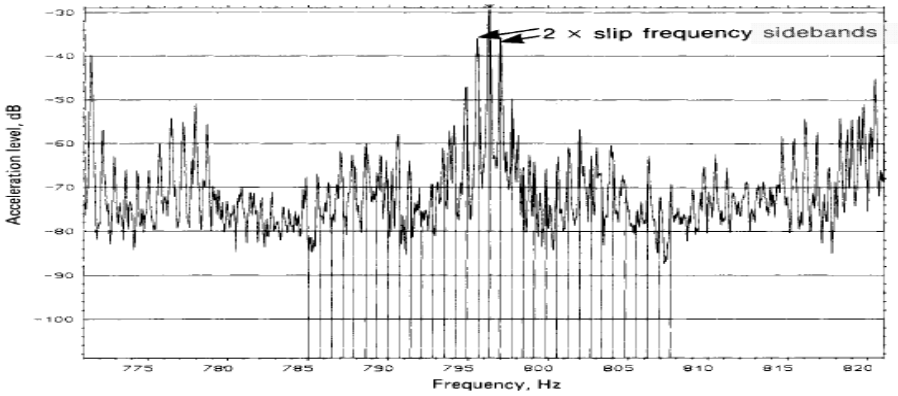

FIGURE 16.6 Zoom spectrum centered around the second principal vibration slot harmonic, showing 2 × slip-frequency sidebands on the component at this frequency.

倒頻譜Cepstrum-1[11]

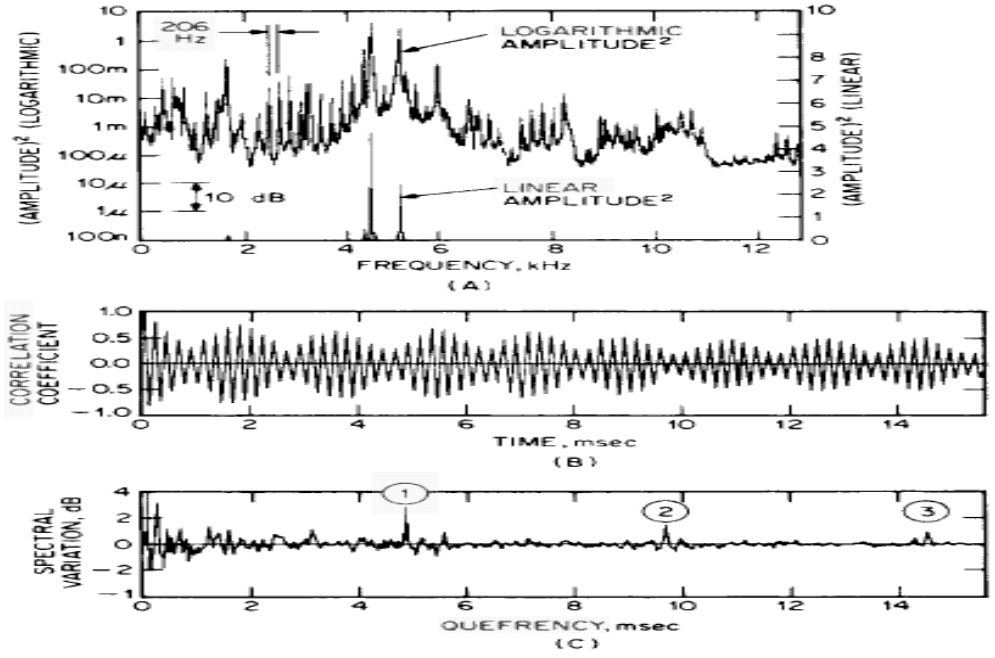

FIGURE 14.31 Effect of linear vs. logarithmic amplitude scale in power spectrum. (*A*) Power spectrum on linear scale (lower curve) and logarithmic scale (upper curve). (*B*) Autocorrelation function (obtained from linear representation). (*C*) Cepstrum (obtained from logarithmic representation)—①, ②, etc., are rahmonics corresponding to harmonic series in spectrum (4.85 milliseconds equivalent to 1/206 Hz). The harmonics result from a fault in a bearing.

倒頻譜Cepstrum-2[11]

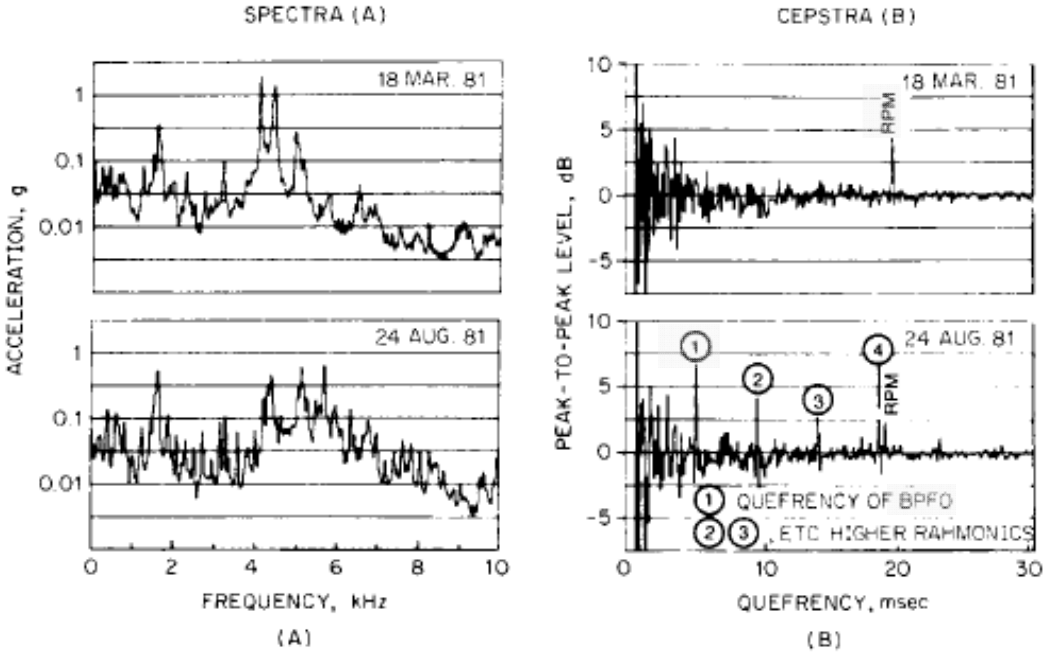

FIGURE 16.11 Analyses of vibration of an auxiliary gearbox before and after the development of a fault on one of the bearings.[10] (*A*) Spectrum analysis; (*B*) the corresponding cepstrum analysis.

包絡分析[11]

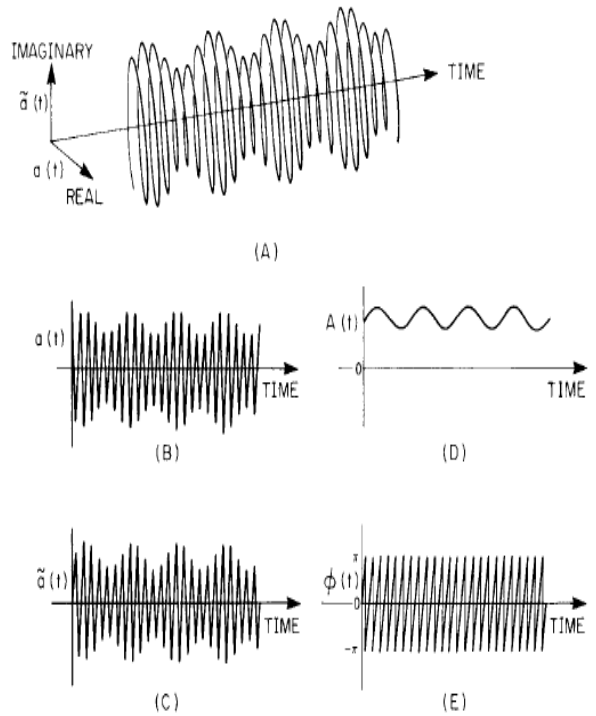

FIGURE 14.33 Analytic signal for simple amplitude modulation. (*A*) Analytic signal $a(t) + j\tilde{a}(t) = A(t)e^{j\phi(t)}$. (*B*) Real part $a(t)$. (*C*) Imaginary part $\tilde{a}(t)$. (*D*) Amplitude $A(t)$. (*E*) Phase $\phi(t)$.

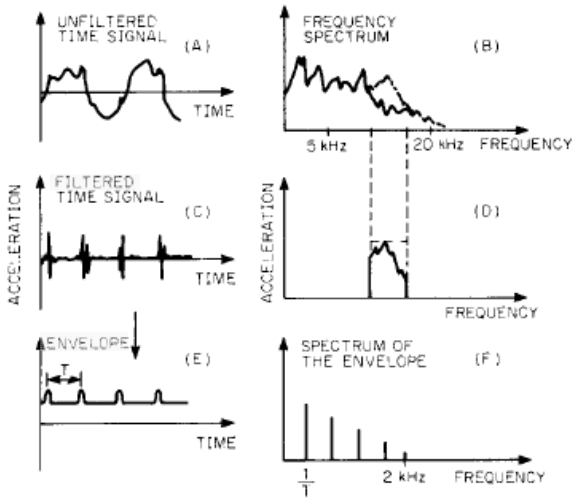

FIGURE 16.9 Principle of analog envelope detection applied to the analysis of impacts due to rolling-element bearing faults. (*A*) *Unfiltered time signal.* (*B*) *The corresponding spectrum in the frequency domain.* (The dotted spectrum represents the reference spectrum before the fault developed. Note the broadband increase due to excitation of a resonance by the bearing fault.) (*C*) *Frequency spectrum after application of a bandpass filter* in range where the change caused by a ball-bearing fault has been detected. (*D*) *Time signal which corresponds with C;* contains ringing of a resonance which is excited periodically. (*E*) Envelope of time signal from *D*. (*F*) *Low-frequency analysis of the envelope from E,* yielding the impact rate due to the fault.

機械故障原因百分比[8]

Imbalance	40%
Misalignment	30%
Resonance	20%
Belts and Pulleys	30%
Bearings	10%
Motor Vibration	8%
Pump Cavitation	5%

偏心振動[12]

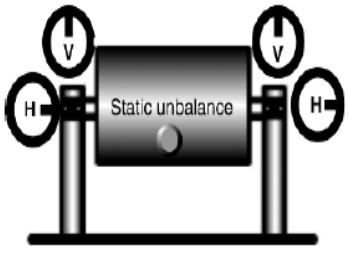

Figure 5.2
Phase relationship – static unbalance

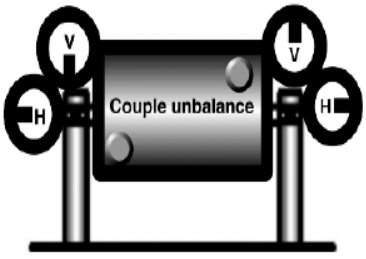

Figure 5.3
Phase relationship – couple unbalance

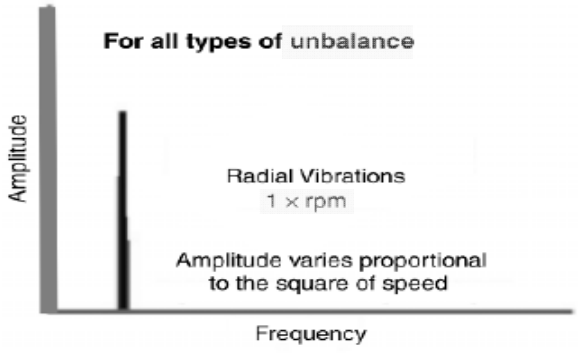

Figure 5.1
FFT analysis – unbalance defect

偏心激振[12]

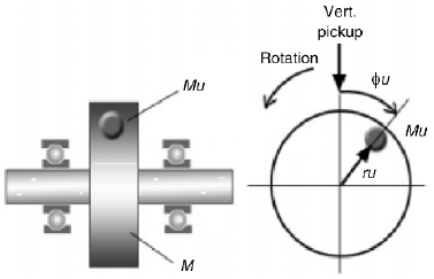

Figure 5.27
A simple rotor system

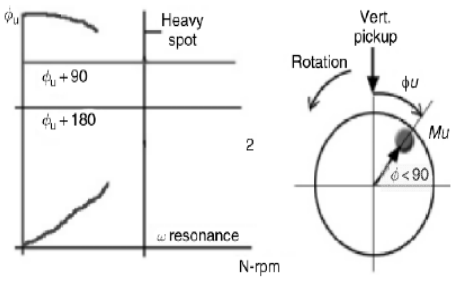

Figure 5.31
Rotor response vs speed increase

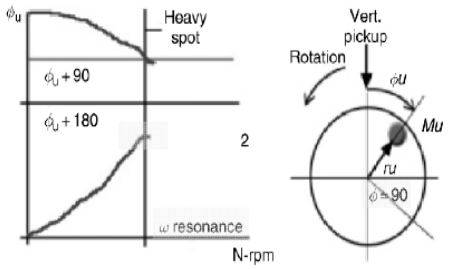

Figure 5.33
Phase relationship at 90°

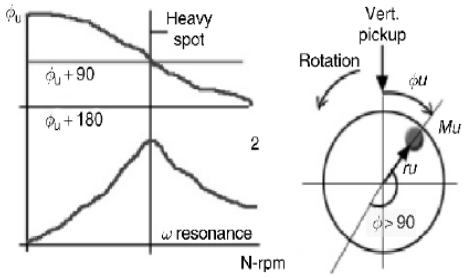

Figure 5.35
Dropping amplitude of rotor vibration

轉軸彎曲變形效應[13]

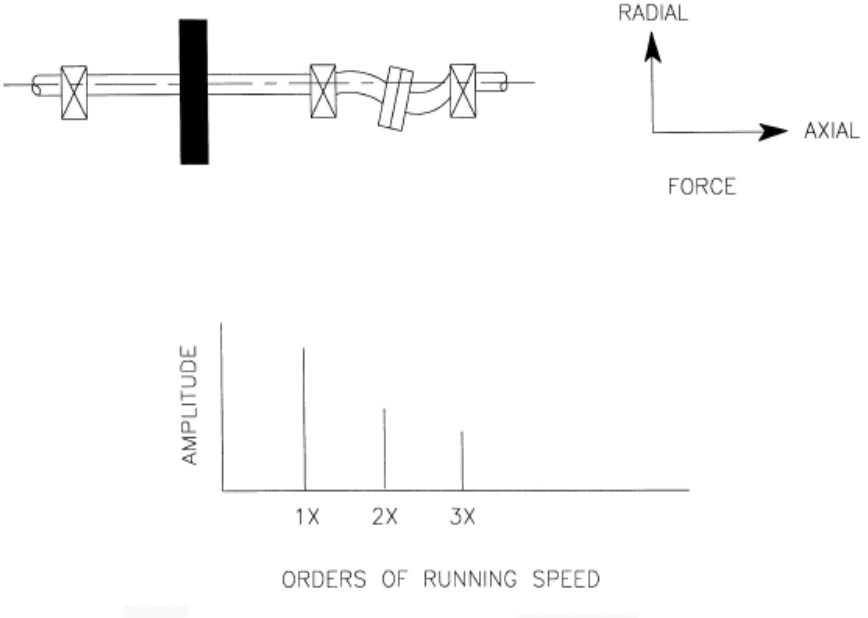

Figure 15.32 Bends that change shaft length generate axial thrust.

轉軸對心問題：角度[12]

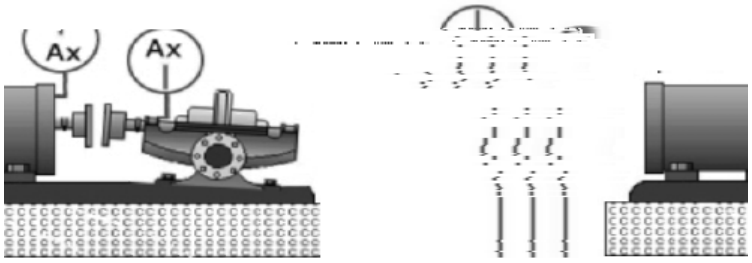

Figure 5.11
Angular misalignment confirmed by phase an

ıalysis

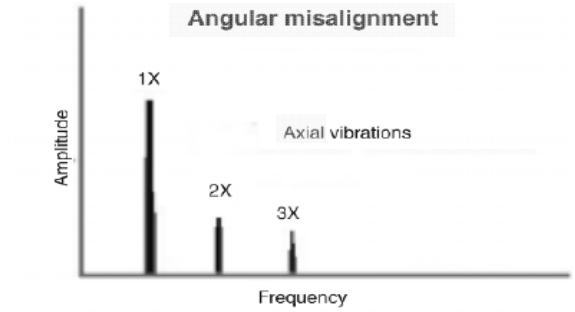

Figure 5.10
FFT of angular misalignment

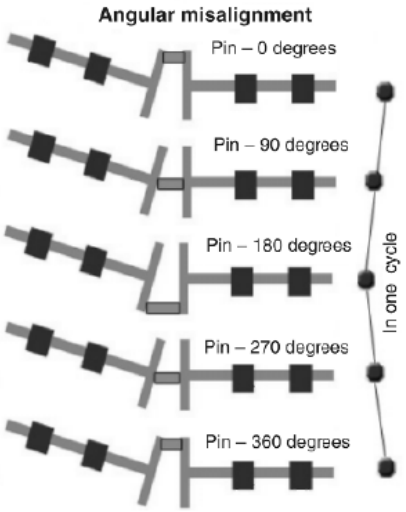

Figure 5.9
Angular misalignment

轉軸對心問題：平行[12]

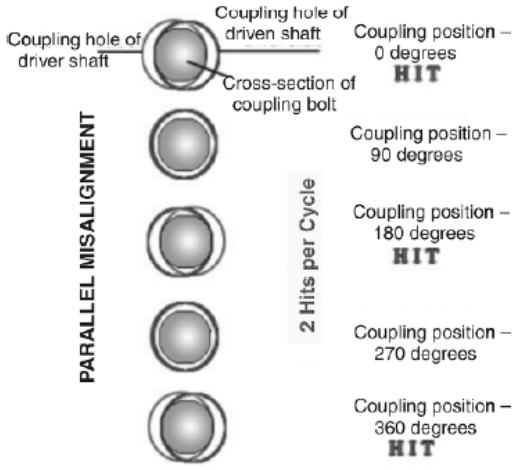

Figure 5.12
Parallel misalignment

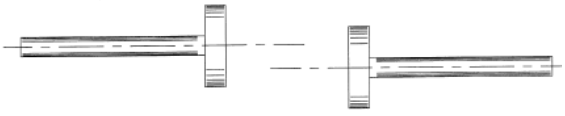

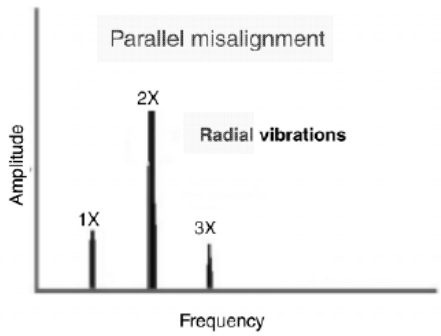

Figure 5.13
FFT of parallel misalignment

鬆脫問題-1[12]

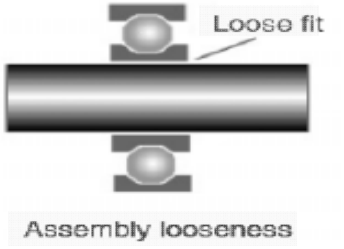

Figure 5.19
Loose fit

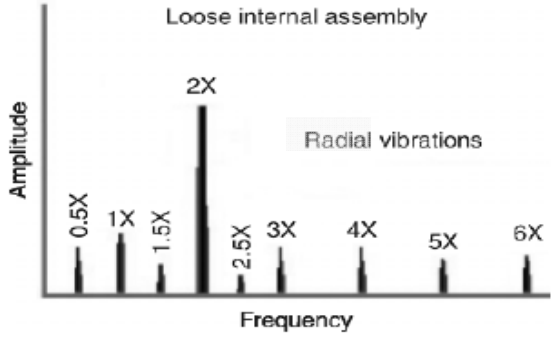

Figure 5.18
Loose internal assembly graph

鬆脫問題-2[12]

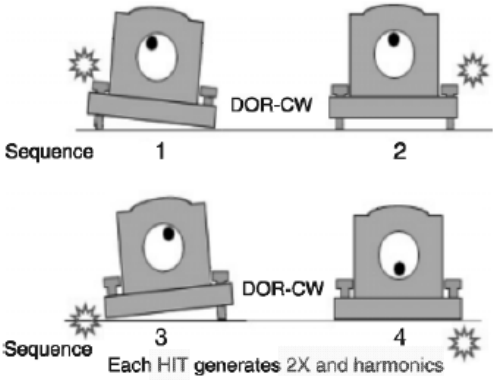

Figure 5.21
Mechanical looseness

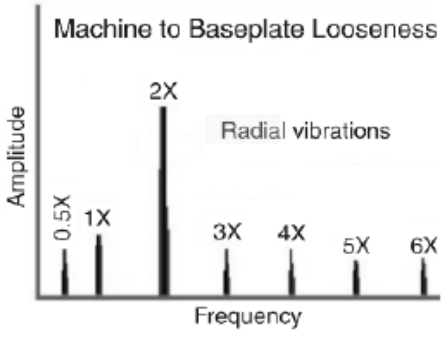

Figure 5.20
Mechanical looseness graph

鬆脫問題-3[12]

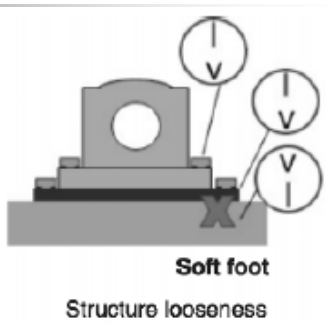

Figure 5.22
Structure looseness

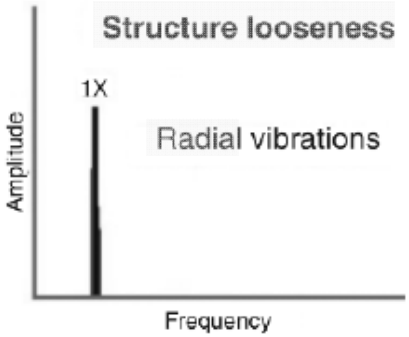

Figure 5.23
Structure looseness graph

轉子摩擦[12]

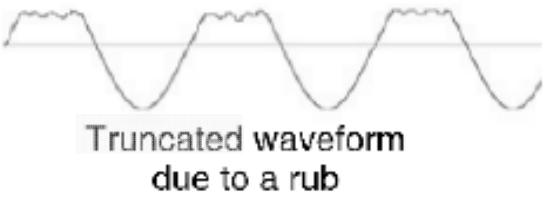

Figure 5.37
Truncated waveform

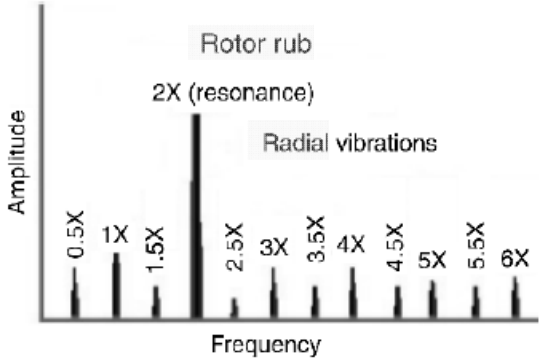

Figure 5.36
Rotor rub

軸承受力不均效應[13]

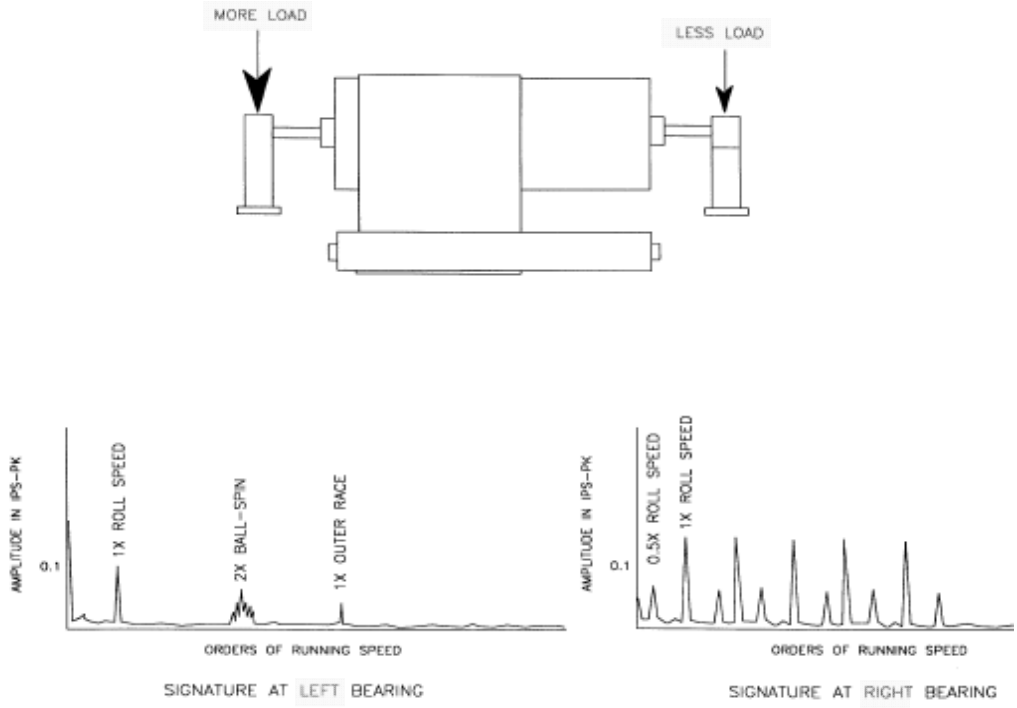

Figure 15.27 Typical vibration profile with uneven loading.

軸承油膜效應[12]

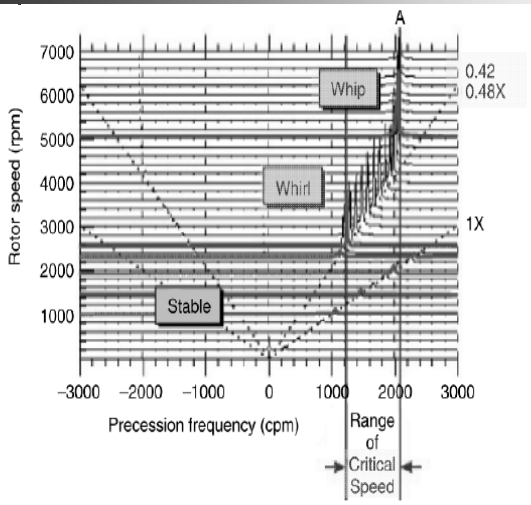

Figure 5.42
Oil whirl/whip as seen in a cascade full spectrum – note the oil whip frequency 'A' getting locked even after raising rotor speed

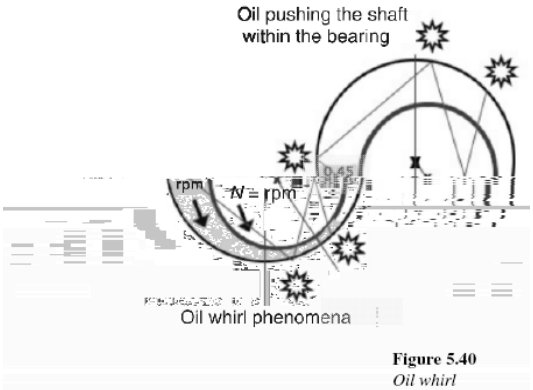

Figure 5.40
Oil whirl

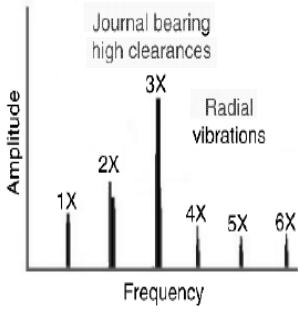

Figure 5.39
High clearance in journal bearings

軸承之振動頻譜[12]

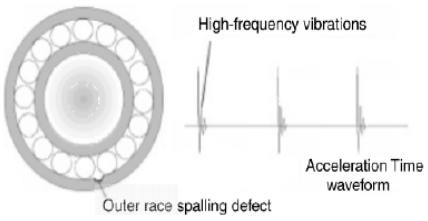

Figure 4.27
Single spalling

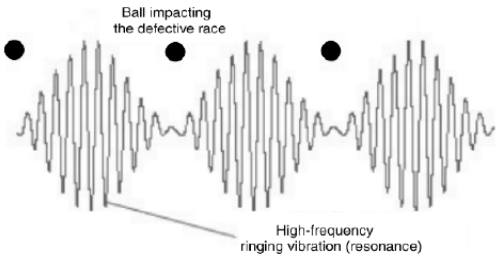

Figure 4.28
Vibration – balls pass over the spall defect

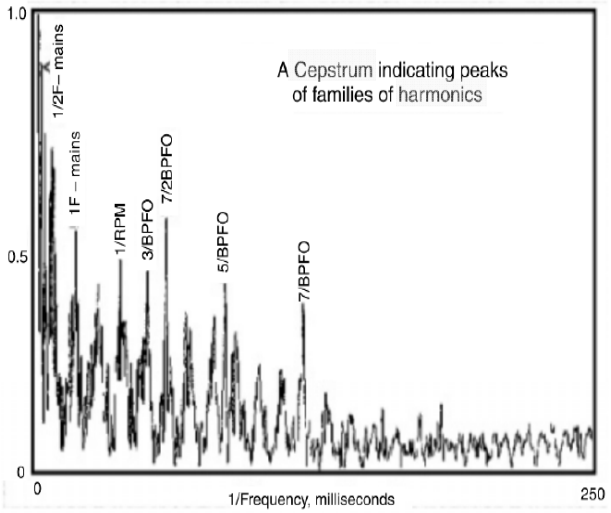

Figure 4.30

軸承磨損效應-1[12]

Zone A: machine rpm and harmonics zone
Zone B: bearing defect frequencies zone (5–30 kcpm)
Zone C: bearing component natural frequencies zone (30–120 kcpm)
Zone D: high-frequency-detection (HFD) zone (beyond 120 kcpm).

$$BPFI = \frac{Nb}{2}\left(1 + \frac{Bd}{Pd}\cos\theta\right) \times \text{rpm}$$

$$BPFO = \frac{Nb}{2}\left(1 - \frac{Bd}{Pd}\cos\theta\right) \times \text{rpm}$$

$$FTF = \frac{1}{2}\left(1 - \frac{Bd}{Pd}\cos\theta\right) \times \text{rpm}$$

$$BSF = \frac{Pd}{2Bd}\left[1 - \left(\frac{Bd}{Pd}\right)^2(\cos\theta)^2\right] \times \text{rpm}$$

Nb = Number of Balls or Rollers
Bd = Ball / Roller diameter (inch or mm)
Pd = Bearing pitch diameter (inch or mm)
θ = Contact angle in degrees

BPFI = Ball pass frequency – Inner
BPFO = Ball pass frequency – Outer
FTF = Fundamental train frequency (Cage)
BSF = Ball spin frequency (rolling element)

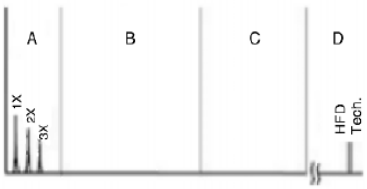

Figure 5.44
Small defects in the raceways of a bearing

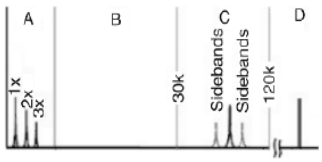

Figure 5.45
More obvious wear in the form of pits

軸承磨損效應-2[12]

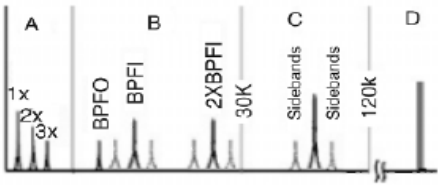

Figure 5.46
Wear is now clearly visible over the breadth of the bearing

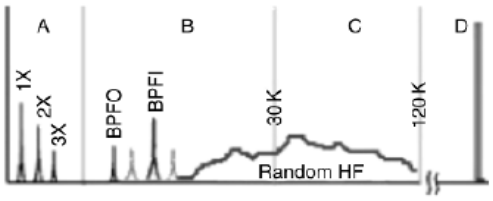

Figure 5.47
Severely damaged bearing in final stage of wear

齒輪振動頻譜-分散式與局部損壞效應[11]

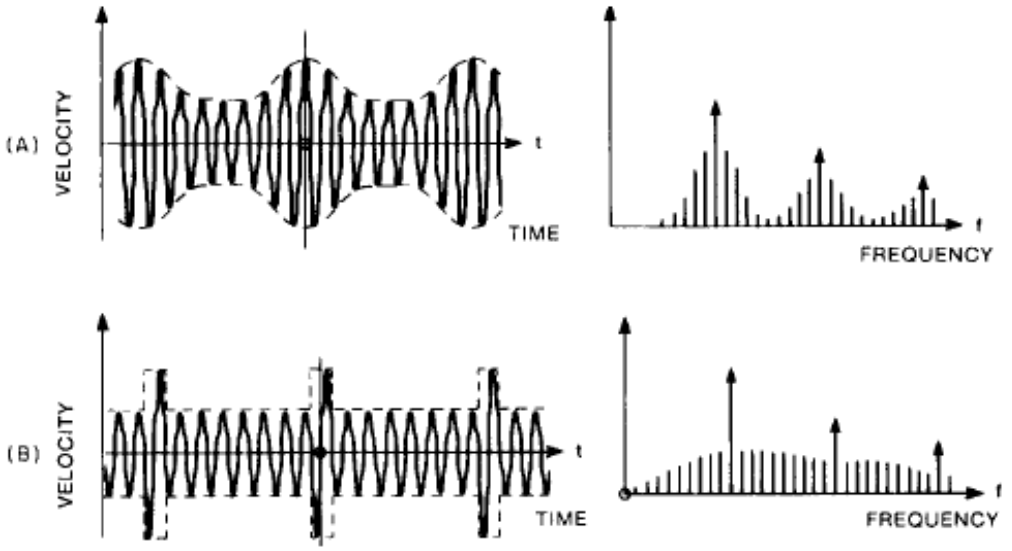

FIGURE 16.7 Distribution of sideband patterns for distributed and local faults on a gear. (*A*) *In the case of a distributed fault,* sidebands have a high level and are grouped around the tooth-meshing frequency and harmonics with a spacing equal to the speed of the faulty gear. The time waveform (lower) shows bursts of energy where the fault passes through the gear meshing area. (*B*) *In the case of a local fault* (such as a cracked or broken tooth), the sidebands have a low level and expand widely over a large frequency range. However, the time waveform shows definite evidence of a chipped tooth. (*Eshleman.*[8])

齒輪振動頻譜-正常狀態[13]

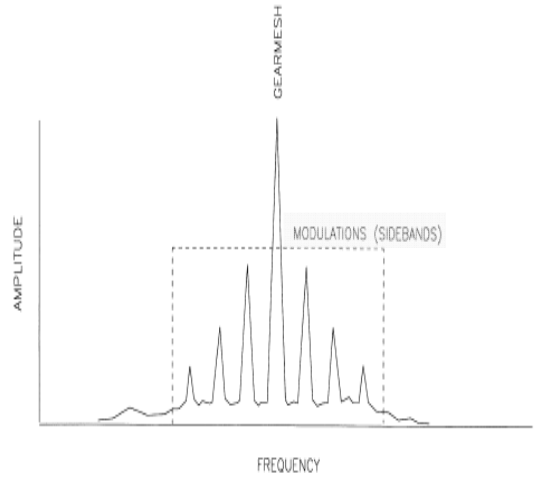

Figure 15.16 Normal gear set profile is symmetrical.

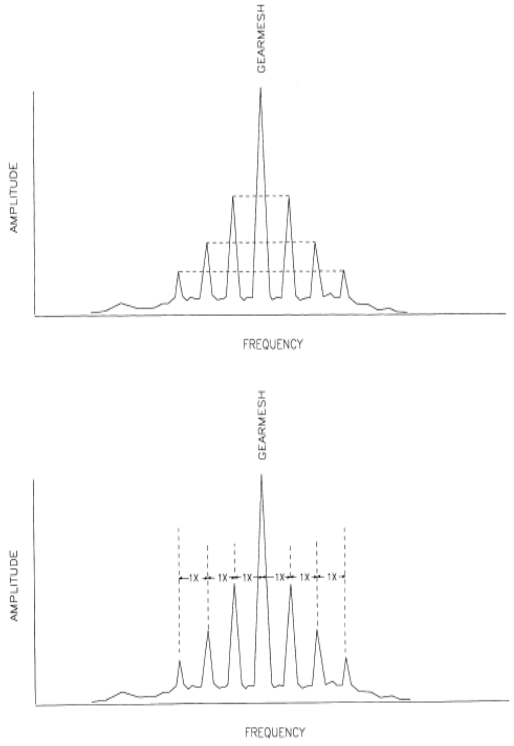

Figure 15.17 Sidebands are paired and equal.

齒輪振動頻譜-異常狀態[13]

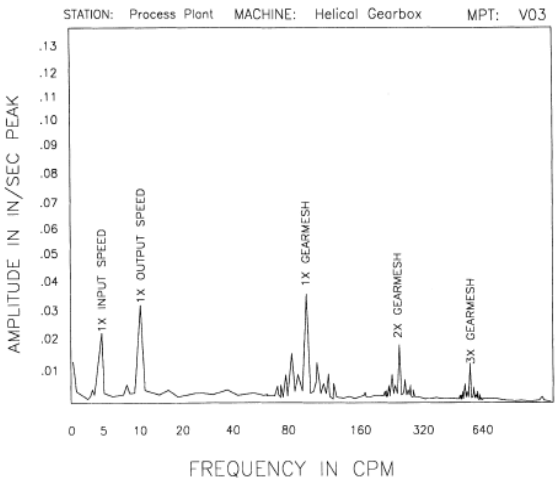

Figure 15.18 Typical defective gear-mesh signature.

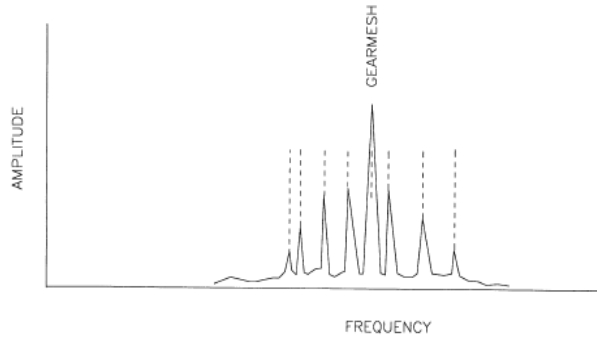

Figure 15.19 Wear or excessive clearance changes the sideband spacing.

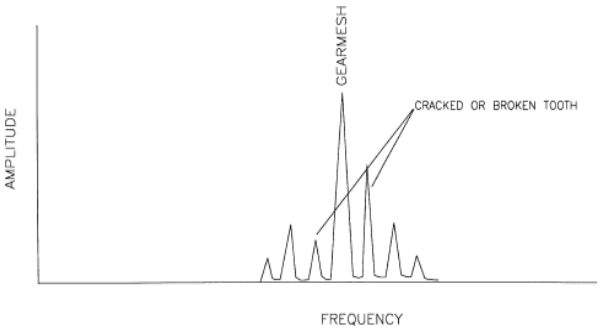

Figure 15.20 A broken tooth will produce an asymmetrical sideband profile.

齒輪磨損與負載效應[12]

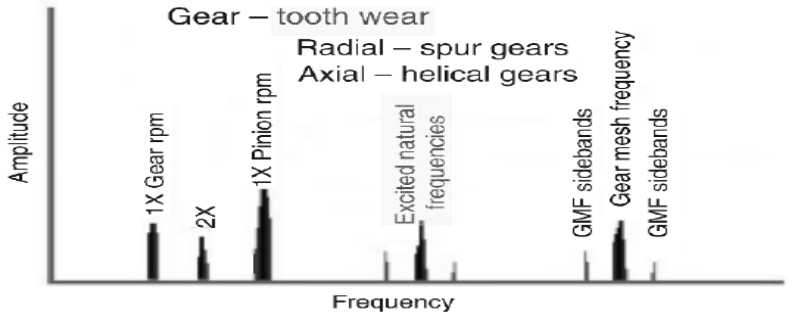

Figure 5.50
Gear tooth wear

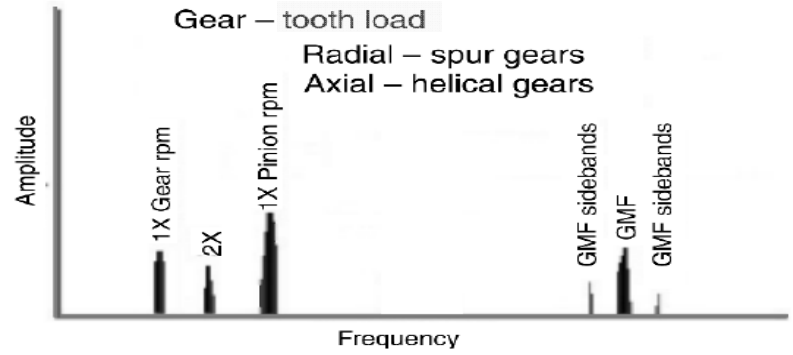

Figure 5.51
Gear tooth load

GMF = number of teeth on pinion × pinion rpm

齒輪背隙與對心效應[12]

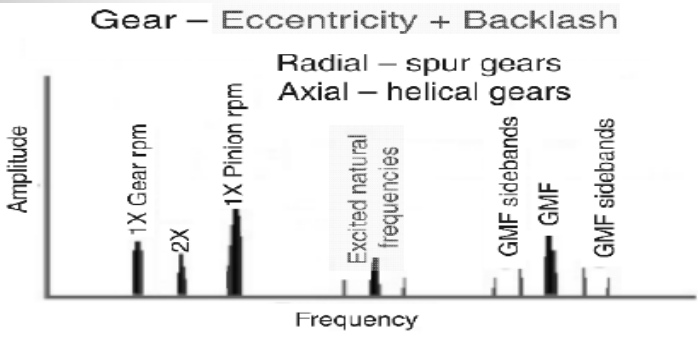

Figure 5.52
Gear eccentricity and backlash

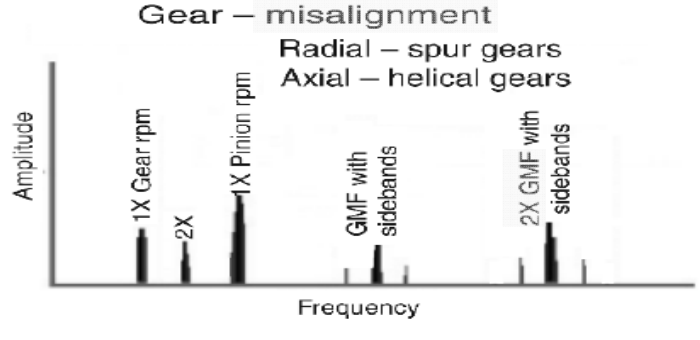

Figure 5.53
Gear misalignment

皮帶輪系統之振動[12, 13]

$$\text{Belt frequency} = \frac{\pi \times \text{pulley rpm} \times \text{pitch dia.}}{\text{belt length}}$$

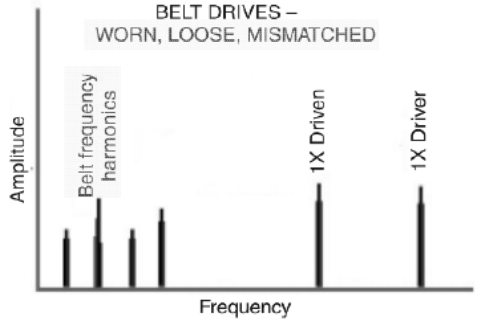

Figure 5.57
Sub-harmonic belt frequencies

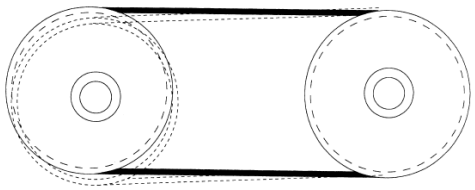

Figure 15.34 Eccentric sheaves.

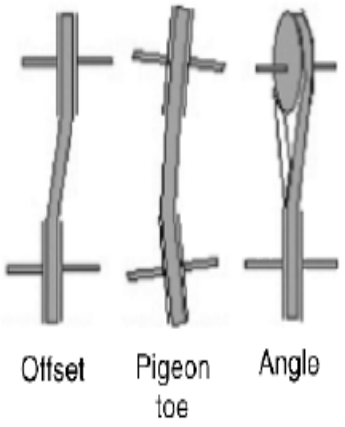

Figure 5.58
Misalignment types (the pigeon toe and angle are classified as angular misalignment)

皮帶輪系統之共振[13]

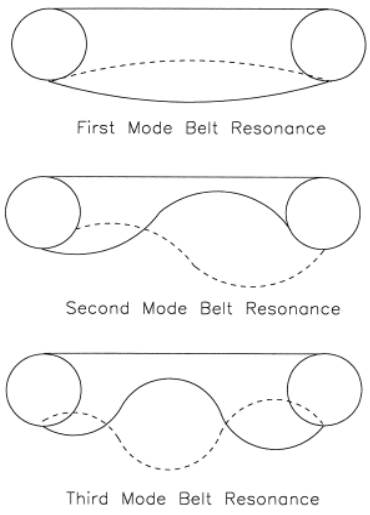

Figure 15.42 Examples of mode resonance in a belt span.

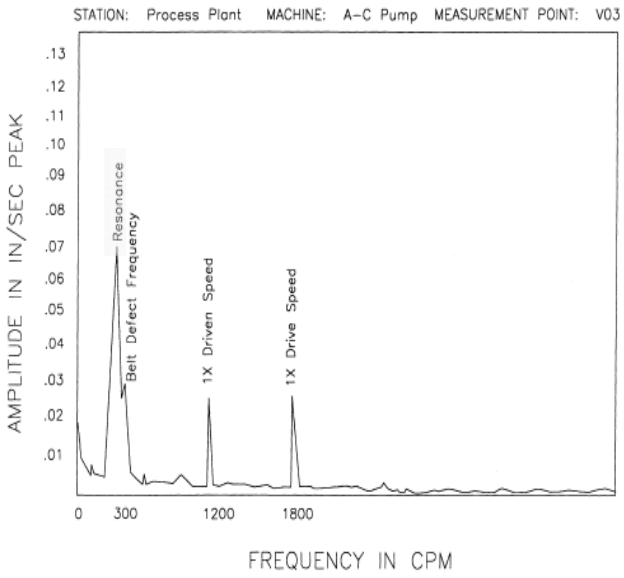

Figure 15.41 Spectral plot of resonance excited by belt-defect frequency.

電力機械振動問題-1[12]

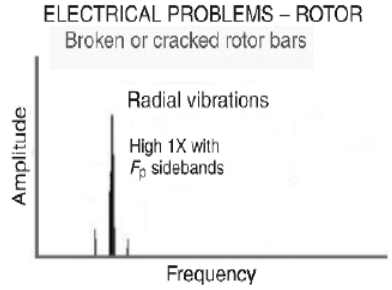

Figure 5.62
High 1× with F_P sidebands

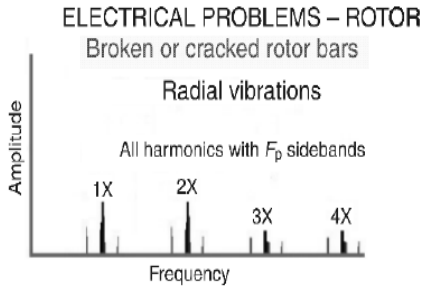

Figure 5.63
All harmonics with F_P sidebands

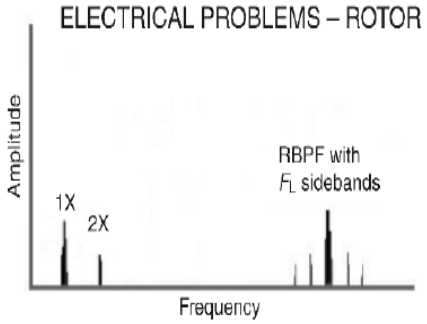

Figure 5.64
Rotor bar pass frequency

RBPF = number of rotor bars × rpm

F_L = electrical line frequency (50/60 Hz)

F_s = slip frequency = $\frac{2 \times F_L}{P}$ – rpm

F_p = pole pass frequency = $F_s \times P$

P = number of poles.

電力機械振動問題-2[12]

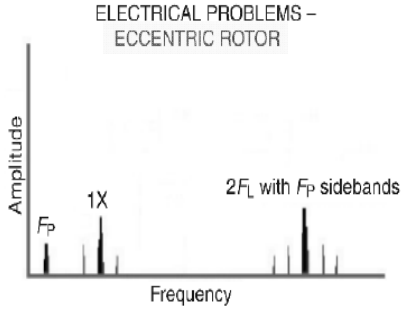

Figure 5.65
Eccentric rotor

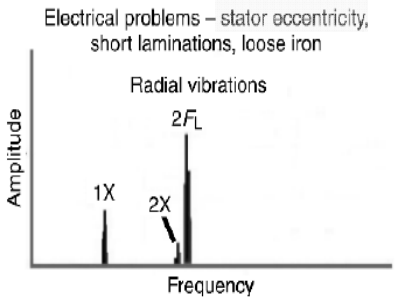

Figure 5.66
Stator defects

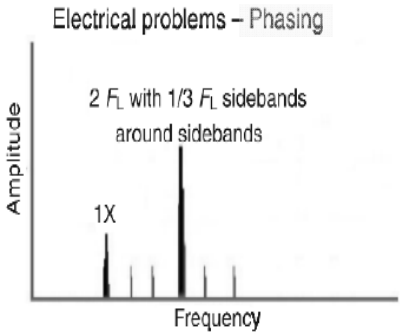

Figure 5.67
Phasing problem

同步馬達振動問題[12]

Synchronous motors (loose stator coils)

Loose stator coils in synchronous motors will generate fairly high vibrations at the coil pass frequency (CPF), defined as:

$$\text{CPF} = \text{number of stator coils} \times \text{rpm}$$

(number of stator coils = poles × number of coils/pole)
The coil pass frequency will be surrounded by 1× rpm sidebands (Figure 5.68).

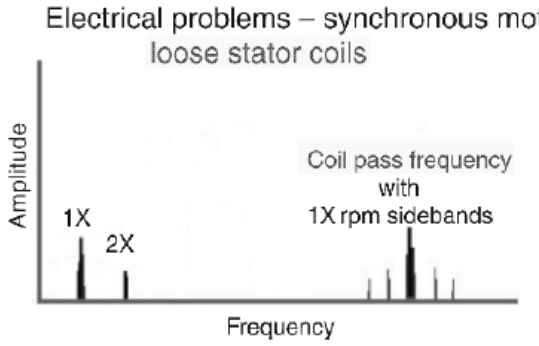

Figure 5.68
Synchronous motors

直流馬達振動問題[12]

DC motor problems

DC motor defects can be detected by high vibration amplitudes at the SCR firing frequency ($6F_L$) and harmonics. These defects include broken field windings, bad SCRs and loose connections (Figure 5.69).

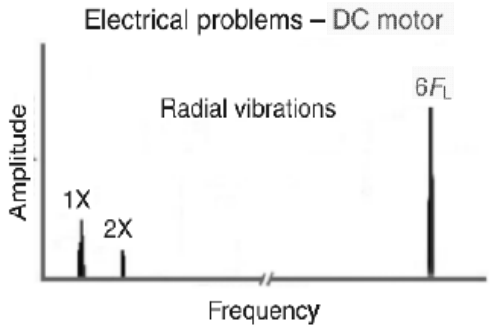

Figure 5.69
DC Motor

Other defects, such as loose or blown fuses and shorted control cards, can cause high amplitude peaks at 1× through 5× line frequency.

流體相關之振動問題-1[12]

Flow-related vibrations

Blade pass and vane pass vibrations

characteristics of pumps and fans.
lot of noise and vibration that can
mponents.

lades (or vanes) × rpm

oblems between the rotor and the
e generated in the pump if the gap
ers is not kept equal all the way

Blade pass or vane pass frequencies (Figure 5.70) are
Usually it is not destructive in itself, but can generate a
be the source of bearing failure and wear of machine co

Blade pass frequency (BPF) = number of b

This frequency is generated mainly due to the gap pr
stator. A large amplitude BPF (and its harmonics) can l
between the rotating vanes and the stationary diffus
around.

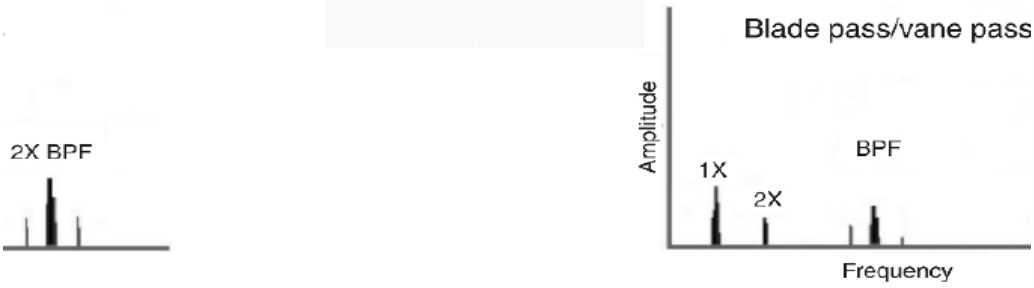

Figure 5.70
Blade pass/vane pass

流體相關之振動問題-2[12]

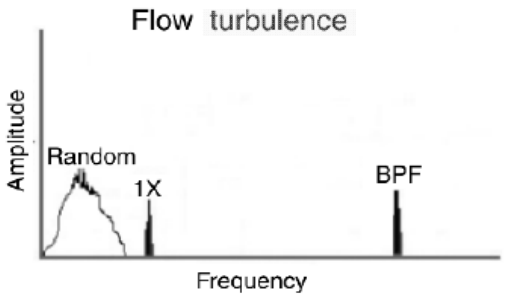

Figure 5.71
Flow turbulence

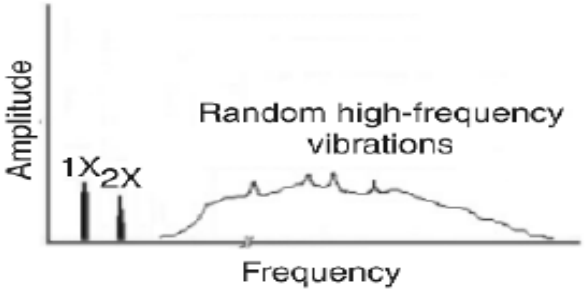

Figure 5.72
Cavitation

旋轉機械之階次頻譜分析[11]

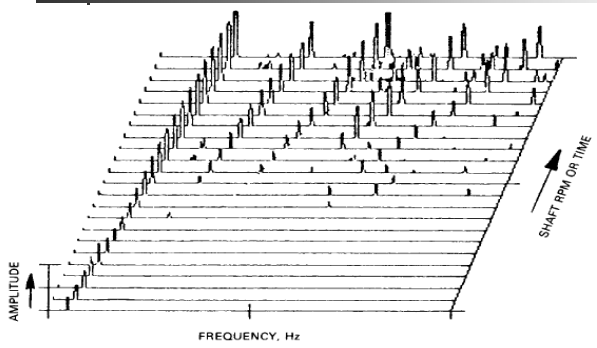

FIGURE 14.25 Three-dimensional spectral map or waterfall plot, showing how spectra change with shaft rpm or time.

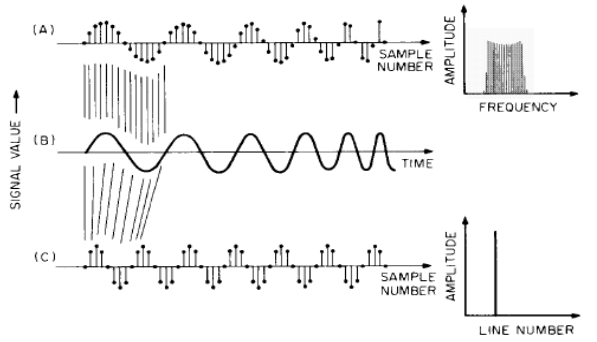

FIGURE 14.26 Analysis of a fundamental component which is increasing in frequency. (*A*) Data record resulting from a uniform sampling rate, and its spectrum, which spreads over a frequency band corresponding to the speed change. (*B*) The original time signal. (*C*) Data record resulting from sampling eight times per fundamental cycle, and its spectrum, which is concentrated in one analysis line.

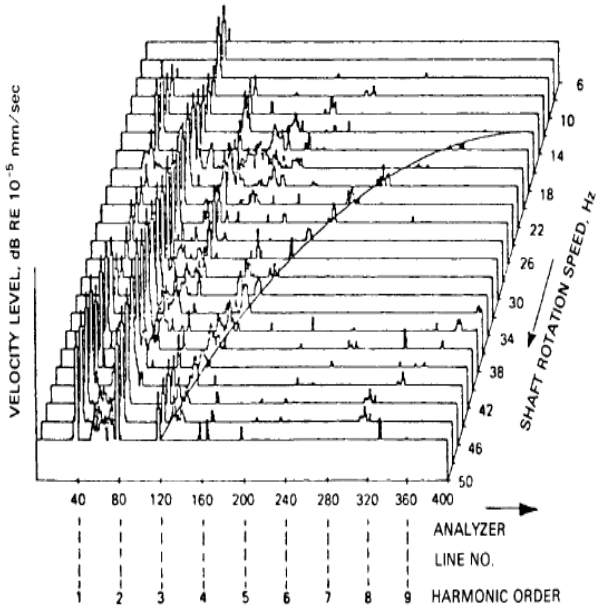

FIGURE 14.29 Tracking FFT analysis of the rundown of a large turbogenerator. The superimposed hyperbolic curve represents a fixed-frequency component at 150 Hz.

變轉速：RPM-Frequency

隨轉速變化：
轉速頻率之倍頻
(嚙合頻)
不隨轉速變化：
共振(自然頻率)
背景噪音/干擾

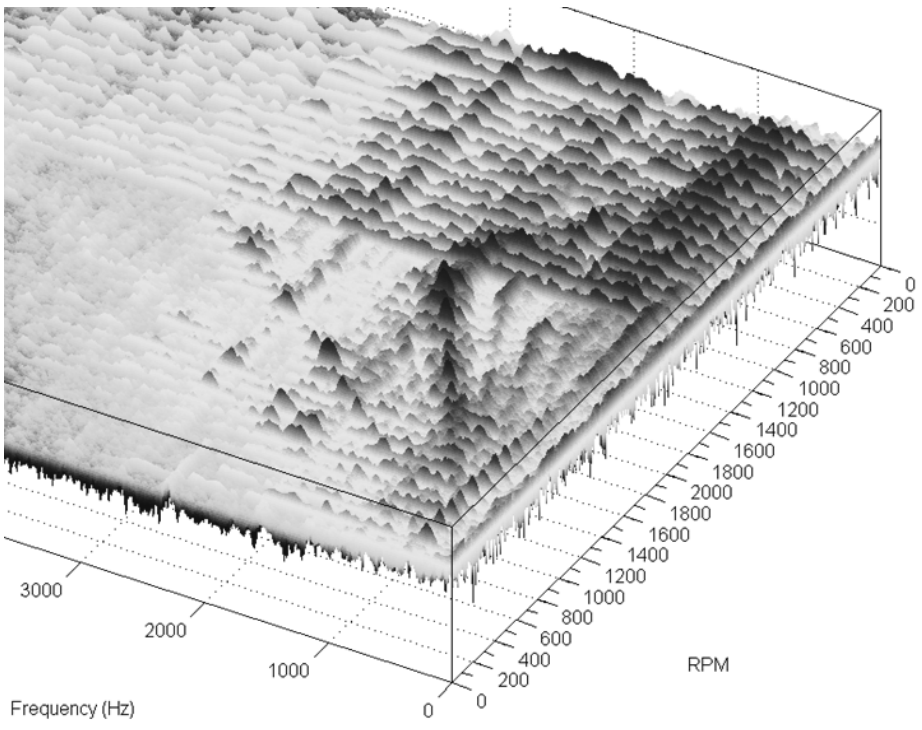

齒輪箱關鍵零組件：模擬⇔量測

FEM模擬結果：

模態	模態形式	自然頻率 (Hz)
12	Coupling	2289
11	Coupling	2176
10	Coupling	2003
9	Coupling	1784
8	Torsion	1541
7	Bending	1421
6	Bending	1415
5	Torsion	1289

量測結果：

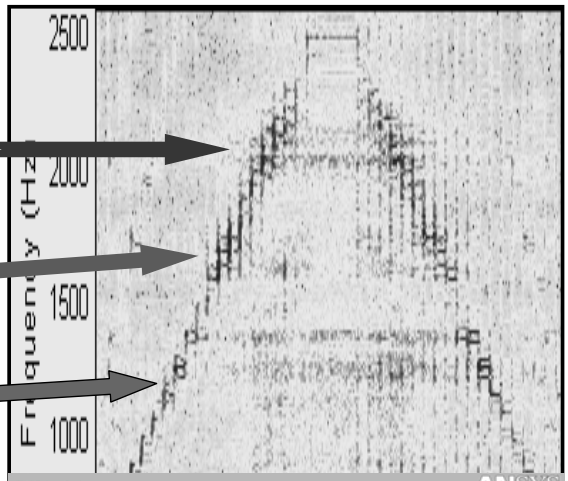

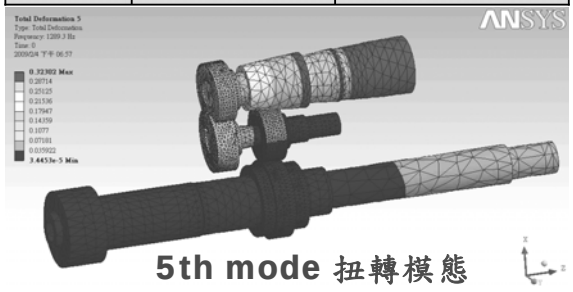

5th mode 扭轉模態

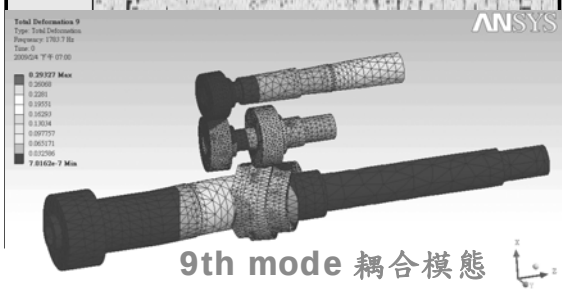

9th mode 耦合模態

高速主軸振動量測：轉速頻率倍頻

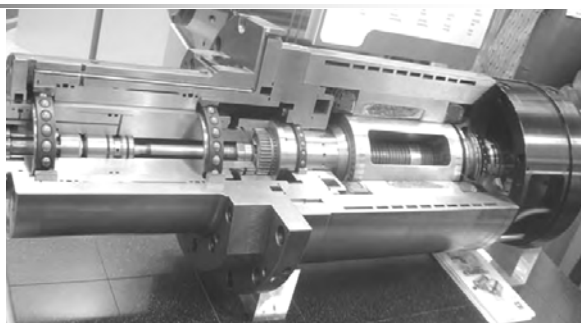

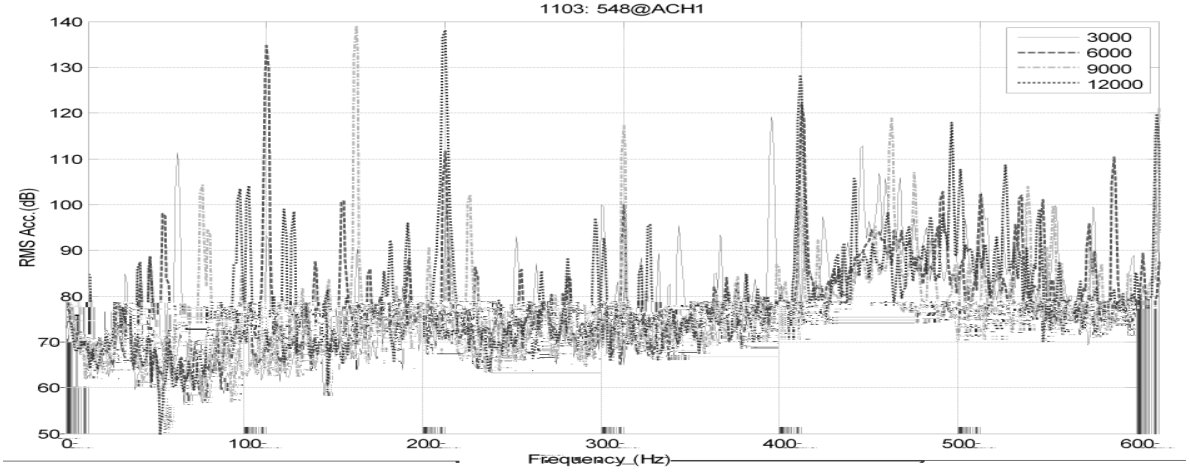

高速主軸振動量測：階次分析

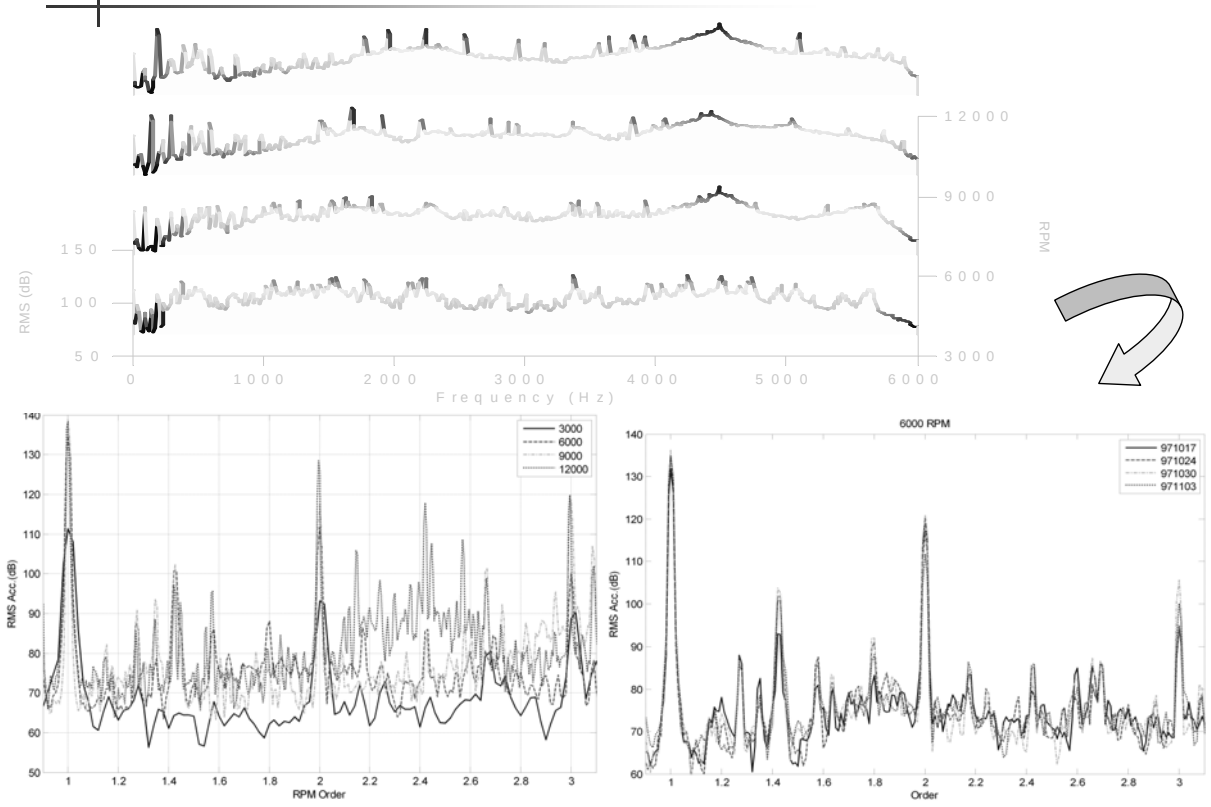

參考資料

1. Austerlitz, H., *Data Acquisition Techniques Using PCs, Second Edition;* Academic Press, San Diego, California, 2003.
2. Bishop, R. H., *Mechatronic System Control, Logic, and Data Acquisition;* CRC Press, Boca Raton, FL, 2008.
3. Cheatle, K. R., *Fundamentals of Test Measurement Instrumentation;* ISA, Research Triangle Park, NC, 2006.
4. Crocker, M. J., *Handbook of Noise and Vibration Control;* John Wiley & Sons, Ltd, Hoboken, New Jersey, 2007.
5. James, K., *PC Interfacing and Data Acquisition: Techniques for Measurement, Instrumentation and Control;* Newnes, Oxford, 2000.
6. Kirianaki, N. V., *Data Acquisition and Signal Processing for Smart Sensors;* John Wiley & Sons, Ltd, New York, NY, 2002.
7. Park, J., *Practical Data Acquisition for Instrumentation and Control Systems;* Newnes, Oxford, 2003.
8. Wilson, J. S., *Sensor Technology Handbook;* Newnes, Oxford, 2005.
9. *Measurements Manual, April 2003 Edition*; Part Number 322661B-01, National Instruments, Austin, TX, 2003.

參考資料

10. A. Muszynska, *Rotordynamics*, CRC Press, New York, 2005.
11. Cyril M. Harris and Allan G. Piersol, *Harris' shock and vibration handbook, Fifth Edition;* The McGraw-Hill Companies, Inc., New York, 2002.
12. Paresh Girdhar, *Practical Machinery Vibration Analysis and Predictive Maintenance;* Newnes, Amsterdam, 2004.
13. R. Keith Mobley, *Vibration Fundamentals;* Newnes, Boston, 1999.
14. Clarence W. de Silva, *Vibration: Fundamentals and Practice;* CRC Press, Boca Raton, 2000.